ML-Driven User Activity-Based GNSS Activation for Power Optimization in Resource-Constrained Environments

Asiimwe Paddy Junior, Luis Enrique Díez, Alfonso Bahillo, and Odongo Steven Eyobu

***Abstract*—The aging population represents an increasing burden on healthcare systems, which is shifting policies from institutionalization to aging in the community. Remote monitoring offers efficient solutions that bridge the gaps between healthcare and where elderly people really want to live every day. However, the adoption of such systems remains low, especially in resource-constrained environments like underdeveloped regions and rural areas, due to the lack of resources often taken for granted in system design. Location is one of the main types of information to monitor, as it provides information about behavior and physical activity. Global Navigation Satellite System (GNSS) is the de facto technology, and although its high-power consumption aligns poorly with battery-powered devices, it is still the best choice for accurate and reliable remote localization of pedestrians. Deciding when to turn on/off the GNSS receiver based on context is a key strategy for power optimization, the two main types of contexts being the user's position and activity. However, existing methods in the literature are not suitable for resource-constrained environments because they require the installation of beacons, which entail additional cost and power consumption, or assume the availability of external signals that are not met in such environments, or are based on simple user activity detection. This work proposes a new GNSS activation method based on detecting the specific walking activity for changing locations. In resource-constrained rural environments, people typically spend most of their time outdoors near their houses, where it is not necessary to activate the GNSS so frequently to monitor them. Restricting the GNSS activation to the moments in which they are moving to a different location could be enough and would reduce the power consumption. Four machine learning (ML) classification models [long short-term memory (LSTM), extreme gradient boosting (XGBoost), support vector machine (SVM), and random forest (RF)] have been implemented and evaluated using a smartwatch's inertial sensor data. The best model, XGBoost, was exported to a custom-designed embedded system and evaluated in real-world tests. It demonstrated over 40% power savings compared to conventional motion-based methods.**

***Index Terms*—Global Navigation Satellite System (GNSS) activation, inertial sensors, localization, machine learning, positioning, power optimization, resource-constrained environment, tracking, user activity.**

Received 27 March 2025; revised 27 June 2025; accepted 21 July 2025. Date of publication 11 August 2025; date of current version 21 August 2025. This work was supported in part by the European Union's Horizon 2020 Research and Innovation Program through the MarieSkłodowska-Curie Grant 847624; in part by REPNIN++ under Grant RED2022-134355-T; in part by the Spanish Ministry of Science, Innovation, and Universities through the AGINPLACE Project funded by MICIU/AEI/10.13039/501100011033 and FEDER, UE, under Grant PID2023-146254OA-C44 and Grant PID2023-146254OB-C41; and in part by the Government of Uganda through the Makerere University Research Innovation Fund (RIF) and CoCIS. The Associate Editor coordinating the review process was Dr. Yulong Huang. *(Corresponding author: Asiimwe Paddy Junior.)*

Asiimwe Paddy Junior is with the Faculty of Engineering, University of Deusto, 48007 Bilbao, Spain, and also with the Geospatial Data and Computational Intelligence Laboratory, School of Computing and Informatics Technology, Makerere University, Kampala, Uganda (e-mail: pjasiimwe@deusto.es).

Luis Enrique Díez is with the Faculty of Engineering, University of Deusto, 48007 Bilbao, Spain (e-mail: luis.enrique.diez@deusto.es).

Alfonso Bahillo is with the Department of Signal Theory and Communications, Universidad de Valladolid, Campus Miguel Delibes, 47011 Valladolid, Spain (e-mail: alfonso.bahillo@uva.es).

Odongo Steven Eyobu is with the Geospatial Data and Computational Intelligence Laboratory, School of Computing and Informatics Technology, Makerere University, Kampala, Uganda (e-mail: odongo.eyobu@mak.ac.ug).

Digital Object Identifier 10.1109/TIM.2025.3597626

I. Introduction

THE most formidable demographic challenge facing the world is no longer rapid population growth but population aging [1]. The number of people aged 65 years and above will double that of children under five, owing to declining fertility, increasing longevity, and the progression of large cohorts into older ages. The trend of an increasing population in older age groups initially began in more economically developed nations, but it is now also evident in low- and middle-income resource-constrained countries. By the year 2050, projections indicate that around two-thirds of the global population aged 60 and over will be concentrated in resource-constrained lower and middle-income nations [2].

The steady rise in the elderly population is likely to place increased strain on families, healthcare, and social services. This is because old age comes with noncommunicable diseases like diabetes, cardiovascular diseases, cancer, and hypertension [3], but also cognitive impairments like dementia that prevent many elderly people from living independently without assistance from a caregiver. For example, several studies [4] show that people with dementia are at least 60% likely to wander in open areas, which exposes them to the potential dangers that are of concern to caregivers.

Aging in place, defined as remaining in a community-based dwelling during one's late years in life [5], is preferred by the great majority of older people and can bring a host of psychological and physical benefits, as well as save costs. As per a 2021 survey conducted by the American Association of Retired Persons, 77% of adults over 50 years would prefer to age in place if given the choice, even when ongoing assistance and healthcare are needed [6]. Thus, healthcare policy should shift from institutionalization to aging in the community to

Fig. 1. Traditional house in rural Uganda.

save costs and provide better care. However, this strategy shifts the burden of care to community-based caregivers who, especially in resource-constrained environments in third-world countries, are predominantly family members and provide most long-term care without any organized training or support [7].

As such, the demand for technologies to meet the critical service needs of the aging population is rising. Remote monitoring solutions utilizing noninvasive, nonintrusive actuators, wearable sensors, and communication and information technologies offer efficient solutions. These technologies bridge the gaps between healthcare and where elderly people prefer to live every day [8]. Such technologies, when implemented correctly, will not only ensure an appropriate quality of life among the elderly persons in their homes but also assist the family and caregivers in providing adequate services to these older adults in society more easily [9].

Multiple remote monitoring systems exist on the market, but the rate at which these platforms have been adopted is extremely low, more so in less developed countries and rural areas. One of the main reasons is the lack or scarcity of resources that these remote monitoring systems take for granted. These systems assume the availability of infrastructure and resources like the Internet, Wi-Fi, cellular networks, and reliable power supply (grid) access. Essentially, they are designed for developed nations (highly technologically resourced environments), but are very much needed in resource-constrained environments as well.

For example, in rural areas of developing countries like Uganda, elderly people commonly live in traditional homesteads characterized by limited infrastructure, primarily in grass-thatched huts, as shown in Fig. 1. Unlike in urban areas, they spend most of their time outdoors, sitting under trees, tending small gardens, or socializing with neighbors. Essential facilities, including toilets and bathrooms, are located outside, requiring frequent walking, and their daily movement is almost entirely on foot. Most elderly residents in these remote areas have never owned a smartphone, primarily because they cannot afford one, and even if they could, the weak cellular network coverage in their area would make it difficult to use reliably, requiring people to move to higher ground or specific spots for a signal just to make calls [10]. In addition, most have never learned how to operate a smartphone due to a lack of exposure and training opportunities, and thus, traditional communication methods, such as face-to-face visits, remain predominant in these communities. The migration of younger, educated family members to urban centers miles away for work leaves elderly parents behind with limited direct family support and supervision, worsening their isolation. Access to essential services is severely restricted. Electricity is unavailable, forcing residents to walk several kilometers to trading centers to recharge devices (mobile phones), often just once a week (in this context, excessive power consumption directly undermines the practicality of remote monitoring systems, as frequent recharging is logistically challenging and costly for users with limited financial resources and mobility). Healthcare services are distant and costly, making regular checkups rare. Financial limitations further hinder the adoption of technology, making it difficult for families to monitor and ensure the safety of their elderly relatives remotely. As a result, existing remote monitoring solutions remain largely inaccessible in such environments despite their potential to address these critical challenges. Therefore, this work aims to contribute to making visible the need to design systems that are suitable for this type of environment.

These remote monitoring tools can collect many different types of information, but among all of them, we will focus on location information, as this can help us to remotely monitor the elderly person's location but also behavior, and infer some basic physical activity information related to the health status (step counter, walking speed, and fall detection) [11].

Although Global Navigation Satellite System (GNSS) is the de facto technology for outdoor localization, it is known to consume relatively high amounts of power, which aligns poorly with the stringent constraints of battery-powered devices. However, as highlighted by the systematic and comprehensive review of the literature in [12] on current pedestrian monitoring systems designed for environments with limited resources, GNSS technology is still the best choice for accurate and reliable remote localization of pedestrians. Consequently, research should focus on mitigating the challenges of GNSS instead of discontinuing its use in resource-limited environments.

Various strategies for optimizing GNSS power consumption have been implemented to extend the lifetime (extend device usability) of IoT devices [13]. Among them, this work will focus on deciding when to activate or deactivate the GNSS receiver according to our user context. Other techniques are available only in expensive GNSS receivers or depend on a reliable communication channel to access the Internet with adequate data rates and capacity, which are often lacking in environments with limited resources, making the implementation of these strategies more challenging in such settings. Our use case and objective are to minimize power consumption by activating the GNSS receiver only when the user is going to change their location significantly.

There are two main types of context triggers: the user position and the user activity. The former is usually based on installing beacons to detect places where it is unnecessary to activate the GNSS receiver. This option is unsuitable for resource-constrained environments because it requires an additional cost and power supply. The latter is usually based on detecting moving or walking activity. Although this approach may function well for objects that are stationary or altering their location, like cars and bikes, it may not effectively optimize power when applied to human users. This is because humans naturally demonstrate frequent movements that can be easily detected and misinterpreted as activities that require the GNSS receiver to be activated, leading to false alarms. In addition, common daily movements, such as short walks within the homestead to outdoor toilets, bathrooms, or nearby gardens, can easily be misclassified as significant mobility, unnecessarily triggering GNSS.

In our opinion, GNSS activation in resource-constrained environments requires an approach that is more intelligent than merely monitoring user acceleration, yet is more cost-effective than implementing beacons. Given that elderly individuals in these settings spend the majority of their time outdoors around their homes, where it is unnecessary to activate the GNSS so frequently to monitor them [14]. Restricting the GNSS activation to the moments in which they are moving to a different location could be enough and would reduce the power consumption. For that, it is necessary to distinguish the shorter and more chaotic walking associated with in-home activities from the longer and more regular walking associated with a translation.

Therefore, this article introduces a novel ML-driven GNSS activation method that triggers GNSS only when it explicitly detects the "walking away" activity class, distinguishing actual departures from home from routine household movements—an aspect overlooked in previous works. Unlike conventional methods that rely on motion thresholds, costly beacon installations, or human activity recognition (HAR) models, which focus on general movement states, the proposed system is designed to operate effectively in resource-limited settings without requiring additional infrastructure. This distinction is particularly relevant and essential for applications intended for elderly monitoring in rural resource-constrained environments, where GNSS activation should only occur when a person genuinely leaves their usual environment. The key contributions of this article are as follows.

1) An optimized GNSS activation method based on detecting the "walking away" activity.
2) An evaluation of four machine learning models—long short-term memory (LSTM), extreme gradient boosting (XGBoost), support vector machine (SVM), and random forest (RF)—highlighting tradeoffs between accuracy and computational efficiency.
3) A real-world validation of a built low-resource embedded system based on our proposed GNSS activation method in a rural, resource-constrained setting, demonstrating over 40% power savings compared to existing methods.

The rest of this article is organized as follows. Section II discusses relevant work related to the state of the art. Section III describes the proposed methodology and materials. Section IV presents details about the experiments, their results, and discussion. Finally, this work is summarized and concluded in Section V.

II. Related Work

The update rate, which can be defined as the frequency with which the positions are calculated on the device or at an external processing facility, or the time interval between two position calculations, should be the first thing to consider when seeking to reduce a receiver's power consumption. This is because GNSS receivers' power consumption is essentially related to user requirements. For example, most GNSS receivers in continuous tracking mode support 10 Hz or even higher update rates [13]. However, some everyday use cases, like tracking pedestrians or elderly people around homes, like in our user case, only require position updates on request or at the event. So, by reducing the update rate to meet a use case's actual requirements and allowing it to enter power save mode between updates, the GNSS receiver can dramatically reduce its power demand.

Different studies have used several methods to activate the GNSS. These methods can be categorized as user-position-based and activity-based, although many studies combine both. Next, we will review some of these works and discuss their suitability for resource-constrained environments.

A. Position-Based Methods

This approach leverages the user's location to reduce unnecessary user position updates and/or GNSS activations. Beacons like Zigbee, Bluetooth, and infrared devices are often installed at users' homes to estimate their position, usually through proximity detection. For instance, in [15], Bluetooth beacons, GNSS signal strength, and an accelerometer were used to detect periods of inactivity, determine if the user was indoors, and subsequently turn off the GNSS. It is worth noting that installing beacons is often impractical for many resource-constrained environments due to the associated costs and the characteristics of the local housing structures in these areas, as demonstrated in Fig. 1. Furthermore, GNSS receivers can maintain a strong signal even when the user is indoors due to the materials, nature, and design of these houses.

Zhang et al. [16] designed an energy-efficient location tracking service, SensTrack, which provides the user's moving trajectory while reducing its impact on the device's battery life. SensTrack smartly selects the location sensing methods between Wi-Fi and GPS and reduces the sampling rate and the time the GPS receiver needs to be activated by utilizing the information from the acceleration and orientation sensors, two of the most common smartphone sensors today. This is done by turning off the GPS when there is no signal and when indoors, and Wi-Fi is then used for localization, also reducing the sampling rate. Like in [15], signal strength may not be an excellent method to determine whether the user is indoors, more so in resource-constrained environments.

Several other works have explored machine learning (ML) techniques to determine if the user position is indoor or outdoor. Abghari et al. [17] used a clustering technique known as inductive system monitoring (ISM) to build a GNSS component activation mode by detecting indoor/outdoor scenarios using LTE cellular signal strength. Zhu et al. [18] leveraged GNSS measurements from Android smartphones to detect indoor/outdoor complex environments. Supervised ML algorithms are then used to predict indoor/outdoor status, which is interpreted as the observations of the hidden Markov model to detect the user transition between indoor/outdoor in complex scenarios. It is important to note that in their work, they just detect indoor or outdoor but do not activate/deactivate GNSS since they need the GNSS signals to make such classification. However, it should be noted that there is limited or no access to cellular networks in most resource-constrained areas, and also, due to the characteristics of the housing materials used in these areas, signal strength outdoors and indoors could be very similar, and thus, their methods may not work effectively.

Junior et al. [19] introduced a position-based method that utilizes a pedestrian dead reckoning (PDR) system. This approach involves setting up a geofence around the user's premises, activating the GNSS only when the individual's calculated position is outside this safe zone (geofence). The experimental evaluations of their work indicate that this activation method provides over 90% greater power efficiency, both outside and within the safe zone, compared to acceleration-based methods, without the need to install any beacons. However, inertial navigation systems for positioning suffer from integration drift. Therefore, relying solely on the individual's relative position, based on the last known position with no corrective measures applied, errors accumulate over time, rendering it ineffective.

B. Activity-Based Methods

In the activity-based approach, various authors [15], [20], [21], [22], [23], [24] have utilized user activity parameters, such as acceleration, velocity, and angular rate, to manage the activation of GNSS and the location update rates.

For example, Paek et al. [25] propose a rate-adaptive positioning system (RAPS) designed to optimize GPS usage in urban environments. RAPS reduces GPS power consumption by activating it only when needed, based on user location history and velocity estimates. It incorporates a duty-cycled accelerometer for movement estimation and Bluetooth for sharing location data among nearby devices to minimize uncertainty. In addition, RAPS uses cell tower RSS blacklisting to avoid GPS activation in areas where GPS signals are likely unavailable, such as indoors. The proposal targets urban environments where GNSS accuracy tends to be lower, thereby necessitating that the GNSS receiver be activated only as frequently as needed to attain the required accuracy. Furthermore, creating a location-time database increases the complexity of the device and raises its communication requirements.

Likewise, Oshin et al. [24] created an accelerometer-based algorithm to accurately identify the individual's mobility state. This innovative algorithm was developed, implemented, and tested on Android-based mobile devices. It was designed to manage the activation and deactivation of smartphone location-sensing technologies such as GPS. Similar to the approach in [25], this method relies solely on acceleration to decide when to activate or deactivate the GPS, which is not particularly effective, especially for pedestrians.

Huang et al. [20] adopted and implemented a method known as the accelerometer-assisted GPS model, originally developed by Oshin et al. [24]. This method employed the built-in three-axis accelerometer to determine whether the user was stationary. To modify the GPS receiver's sampling rate and minimize power consumption, the authors focused on two motion patterns: stationary and movement. When a pedestrian was stationary, the system would suspend GPS sampling for positioning. Conversely, when the pedestrian began to move, the system adjusted the GPS sampling rate based on the correlations between the maximum search range, the service area, and the individual's current location. Their approach considered the individual's position rather than solely the mobility state. The location of a user was assessed in relation to points of interest, such as heritage sites, scenic areas, landmarks, popular shops, or nearby restaurants. To gather this contextual information, pedestrians continuously updated their geographical locations via the cellular network, regardless of whether they were in motion or at rest. Although the authors incorporated the concepts of a geofence and user position, the system's design is not suitable for resource-constrained environments as it relies on network connectivity and reference points, such as popular stores or restaurants, to ascertain the user's location, resources that are typically unavailable in rural, resource-limited settings.

Based on our analysis, existing activity-based GNSS activation methods can be broadly classified into three categories.

1) Acceleration thresholding methods, which rely on a predefined acceleration threshold to activate GNSS. These methods are simple and straightforward, but they result in frequent unnecessary activations for typical home-based movements, thereby saving minimal energy in our scenario.
2) Walking detector methods, which trigger GNSS upon detecting general walking. Current literature typically focuses on generic walking detection without distinguishing the context or specific types of walking (e.g., walking at home versus walking away from home). Typical characteristics examined in these methods include the number of steps per second, walking pace/speed, heading stability, and overall movement intensity.
3) Multiple modes of transport classifiers, designed to differentiate various transportation modes such as walking, cycling, and driving. Although effective in multimodal contexts, these methods are excessively complex for our resource-constrained scenario, where walking is the predominant, if not exclusive, mode of transport.

In contrast to these approaches, we hypothesize that explicitly detecting the activity of "walking away" rather than general walking is possible and sufficient for our use case. This specificity can significantly improve energy efficiency by reducing unnecessary GNSS activations, particularly suited to rural, resource-constrained environments. Importantly, our objective is not to pinpoint precisely the exact second a person leaves home but to maximize energy savings through timely and contextually relevant GNSS activations, leading to meaningful battery-life improvements measured in hours rather than seconds. It should be noted that this is an improvement and contextual adaptation rather than a complete paradigm shift.

In summary, the activity-based method may be effective for objects that are either changing their position or are stationary, such as bikes, but it may not provide an optimal solution for optimizing power in the case of human users, as is the case in our situation. This is because humans naturally display frequent movements that can be easily detected and misinterpreted as activities that necessitate the activation of the GNSS receiver, resulting in incorrect triggers.

C. ML-Based HAR Methods

HAR refers to using ML algorithms and sensor data from various devices to detect and categorize human activities such as walking, running, bathing, and cooking [26]. These activities can be leveraged to estimate the user's position around the home and optimize GNSS activations. HAR is a very active research topic in the field of sensing, pervasive computing, and localization, with many applications in real-world scenarios such as smart environments, health and well-being, surveillance and security, and human–computer interaction [27].

Sensors such as accelerometers, gyroscopes, and magnetometers are commonly used to detect these low-level activities. For example, accelerometer sensors measure dynamic (vibration or movement) and static (e.g., gravity) forces of acceleration acting on the sensor, providing valuable data in detecting user movement patterns (walking speed and step length). The gyroscope sensor measures the angular velocity, i.e., the rate of change of the sensor's orientation, providing information for detecting patterns in user activities that involve rotation around a particular axis. Combining these two inertial (accelerometer and gyroscope) sensors provides a more reliable mechanism to distinguish numerous human activities [27].

Model selection is a crucial aspect of HAR, as it determines the ML algorithm or model used to classify and predict human activities based on the collected sensor data. The choice of model can significantly impact the accuracy and performance of the HAR system. Several studies have recommended using diverse classification models for HAR to leverage their complementary strengths. For example, Bulling et al. [28] and Lara and Labrador [29] recommend the use of LSTM networks for activity classification because their recurrent architecture effectively captures long-term temporal dependencies in sequential sensor data, which is critical for discerning subtle temporal variations in human motion. These properties are particularly valuable when the objective is to distinguish between nuanced activities, such as differentiating "walking at home" from "walking away from home."

Similarly, ensemble methods have gained traction in recent works. For example, Wang et al. [30] and Nweke et al. [31] advocate using ensemble approaches such as XGBoost for activity classification because these methods can model complex nonlinear relationships through gradient boosting. This iterative error-correction mechanism enhances classification accuracy and offers computational efficiency, an essential consideration for deployment on resource-constrained devices. In these studies, XGBoost is praised for its scalability and ability to work effectively with reduced feature sets, as highlighted by using techniques like SHapley Additive exPlanation (SHAP) for feature selection.

Traditional models such as SVM and RF are also recommended in the literature. According to [28] and [31], SVM is favored for generating robust decision boundaries in high-dimensional feature spaces, making it a reliable baseline for many HAR tasks. Concurrently, RF is valued for its classification performance and its inherent ability to provide feature importance metrics, which aid in feature reduction and model interpretability.

Thus, by integrating RF, SVM, XGBoost, and LSTM, our work draws on a spectrum of methodologies that address the challenges of activity classification in low-resource environments while ensuring high accuracy and efficiency in GNSS power optimization.

The feature selection process in this work was driven by the need to accurately capture the nuances of human motion while minimizing computational overhead—an essential requirement for resource-constrained environments. A range of time domain features (including mean, standard deviation (STD), root mean square (rms), and kurtosis) and frequency domain features (including entropy, energy, and skewness) were extracted from the data. HAR studies have widely validated these features for their ability to characterize the dynamic and static properties of inertial sensor signals [27], [28]. To further refine the feature set, we employed SHAP analysis, which allowed us to quantify the contribution of each feature to the model's predictions. This enabled us to identify and retain only the top ten most discriminative features. The resulting reduced feature set helps prevent overfitting by eliminating redundant or less informative data and decreases memory and processing requirements—critical factors for ensuring efficient operation on low-resource devices [32], [33].

Several authors have explored these human activities to determine when to activate the GNSS. For example, Esmaeili Kelishomi et al. [34] proposed an approach to accurately detect the indoor/outdoor environment according to six different daily activities of users, including walking, skipping, jogging, staying, and climbing stairs up and down. Even though classifying the user position as indoor or outdoor might result in better results than just using acceleration, knowing the user is outdoors is not enough information, more so in our user case, as being outdoors does not necessarily mean the user is lost and needs the caretaker's attention. Plus, most users in rural, low-resourced environments spend most of their time outdoors [14]. This will still cause unnecessary GNSS activation. Notably, no existing HAR method specifically detects a "walking away from home" activity class, nor has any previous work proposed a GNSS activation method tailored explicitly for resource-constrained environments based on detecting this specific class.

Overall, the article uses these four models to cover a broad spectrum of ML techniques—from traditional ensemble methods (RF) and kernel-based classifiers (SVM) to advanced ensemble boosting (XGBoost) and deep learning architec-

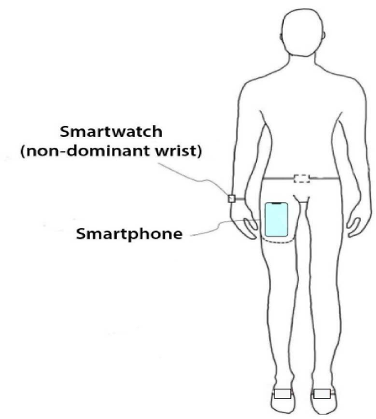

Fig. 2. Experimental setup.

tures (LSTM). This comprehensive evaluation helps identify a model that not only delivers high classification performance but also meets the computational constraints of our embedded system, with XGBoost emerging as the most balanced choice for deployment.

III. Material and Methods

We introduce a novel GNSS activation method based on user activity. The core idea of our proposal is detecting the activity "walking away from home," and this approach harnesses the power of ML to discern between user motion modes at home and when moving to a different location. The differentiation of these user motions is based on primary datasets that characterize different types of movements associated with various home user activities, such as sitting, standing up, walking from one room to another, washing dishes, and so on. Our focus is not on classifying user activities, such as those in HAR, but rather on determining whether the user is walking away from home.

Unlike the methods reviewed in Section II, we hypothesize that detecting the activity of "walking away from home" is sufficient for resource-constrained environments, as this approach eliminates the need for beacons, avoids assumptions about varying signal strengths indoors and outdoors, is better than just basic acceleration signal thresholding, and is simpler than HAR since we do not need to classify different daily user activities.

The objective of this Section III is to present the selection criteria of a classification model that is good enough to be implemented and validated in a real device and experiments. Next, inertial data collection, data preprocessing, feature engineering, and classification model selection will be described, where four common classifiers will be evaluated: RF, LSTM, SVM, and XGBoost.

A. Data Collection

The data collection process was facilitated by sensor logger [35], a free, easy-to-use, cross-platform data logger installed on a smartwatch worn on the nondominant wrist, as illustrated in Fig. 2. This application logged readings at a sampling frequency of 100 Hz from the accelerometer and gyroscope sensors during the experiment. The smartwatch was connected to the smartphone, which served as a data storage device for the recordings captured during the process. The hardware used in this experiment was the iPhone 12 series and an Apple Watch Series 7. We recognize that our system is intended for resource-constrained environments; however, the choice of the hardware for data collection was primarily due to their availability in the lab at the time of the experiments. However, this choice does not impact the generalization of the resultant model when embedded on a low-cost device, as demonstrated in Section IV. For this study, the device on which the model was embedded runs on an ESP32 microcontroller for validation in real-world experiments.

Data was collected in a simple natural home environment to accurately represent user activities in resource-constrained home environments, and as the participant walked away from home to work, to represent movements away from home. For the walk from home to work, participants made short stops to simulate typical everyday situations in the local low-resourced area when the elderly people pause to greet other passersby, a common occurrence in these environments.

Two elderly participants—a female aged 72 and a male aged 70—participated in the data collection process. The experiments were conducted daily for two weeks (ten working days) at their homes. Each day, both participants were recorded for 20 min while performing activities at home, such as sitting, sleeping, washing utensils, standing, or moving from one room to another, and another 20 min while walking away from home (approximately 800 min of recordings). Our ground truth was raw data labeled "at home" and "walking away" from home based on human observation. These classes represented data collected during the user's activities around the home and while walking away from home, respectively.

Inclusion criteria required participants to be older adults (65 years and above) capable of walking unassisted and performing daily activities independently. Exclusion criteria eliminated individuals with severe cognitive impairments (e.g., advanced dementia) or significant physical disabilities (e.g., requiring mobility aids or exhibiting unsteady gait). These criteria ensured that the data reflected the typical gait patterns of independently mobile elderly individuals in resource-constrained settings, thereby minimizing the confounding effects of severe health conditions. While limiting applicability to populations with significant impairments, these criteria align with the target use case of monitoring independently living elderly in rural areas.

B. Data Preprocessing

1) Data Filtering: Most of the energy of the inertial signals during human activity is in the frequency band of 0–20 Hz, as validated by prior HAR studies [36], [37], [38], [39]. Therefore, we filtered the six acceleration and angular rate signals to make the signal segmentation and subsequent computational steps more robust. We applied two zero-phase fifth-order Butterworth filters: one high-pass filter with a cut-off frequency at 0.5 Hz and another low-pass filter with a cut-off frequency at 20 Hz. This 0.5–20-Hz bandpass range was chosen because

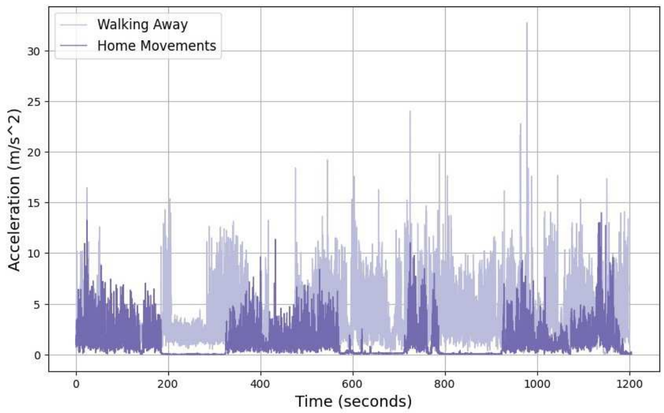

Fig. 3. Presents a visual example of accelerometer magnitude data collected during user activities around the home and while walking away from home.

human gait and daily activity signals predominantly lie within these frequencies. The 0.5-Hz high-pass filter removes very low-frequency components (e.g., gravity-induced drift), while the 20-Hz low-pass filter attenuates high-frequency noise, thereby preserving the relevant motion data. Utilizing a zero-phase fifth-order Butterworth design ensures sharp cutoffs with minimal phase distortion, yielding cleaner inertial signals for reliable segmentation and feature extraction.

2) Signal Vector Magnitude: Each of these sensors provides data in three dimensions: the x-, y-, and z-axis. Orientation changes can impact the recognition performance of these sensors, resulting in a drop in performance if the classification algorithms were trained only for a specific orientation [40]. To mitigate the effects of orientation changes, we added a fourth dimension to each sensor's existing three dimensions, referred to as the sensor's magnitude.

The acceleration vector magnitude is calculated from the acceleration's three orthogonal components (x, y, and z). The formula is

$$a_{\text{mag}} = \sqrt{a_x^2 + a_y^2 + a_z^2} \tag{1}$$

where a_x, a_y, and a_z are the acceleration signals along the x-, y-, and z-axis, respectively.

Similarly, the gyroscope vector magnitude is calculated from the angular velocity's three orthogonal components (x, y, and z). The formula is

$$w_{\text{mag}} = \sqrt{\omega_x^2 + \omega_y^2 + \omega_z^2} \tag{2}$$

where ω_x, ω_y, and ω_z are the angular velocity signals along the x-, y-, and z-axis, respectively.

Magnitude signals are related to the movement intensity as they account for the overall movement. Fig. 3 presents a visual example of accelerometer magnitude data collected during user activities around the home and while walking away from home. It clearly illustrates the difference in movement intensity. The intensity of the accelerometer data is notably higher during the "walking away from home" activity, with frequent peaks reaching up to 30 m/s^2, indicating strong, continuous motion and higher physical effort. Most values remain above 5 m/s^2, showing consistent, vigorous activity typical of walking at a steady or fast pace. In contrast, the "home movements" activity exhibits much lower intensity, with most values between 0 and 10 m/s^2 and only occasional peaks around 10–15 m/s^2, reflecting lighter, intermittent movements such as walking indoors or short, less strenuous actions.

By utilizing the vector magnitude of the accelerometer and gyroscope signals, we minimize errors caused by device orientation and axis-specific biases. The magnitude (an orientation-invariant measure of overall motion) reduces sensitivity to how the device is worn and combines information from all three axes, smoothing out noise or calibration errors that might affect any single-axis reading.

3) Data Segmentation: In order to facilitate effective feature extraction, a fixed-size overlapping sliding window segmentation technique was used. The signals were split into windows of a fixed size of 5 s with a 50% overlap. This was applied to the entire dataset to provide context about the features' behavior over time.

Although a 1–2-s window size has proven to provide the best tradeoff between HAR speed and accuracy [41], in our case, we selected a 5-s window because our experiment was not highly controlled, and the participants did not strictly perform one activity. This implies that data variations based on human participants' gait and motion will ideally represent various activities if a smaller time window is used. Our experiments use data collected in 5 s and are preprocessed and feature-engineered to provide a better generalization for a dominant activity. Also, the models need to better identify subtle variations in the data, which are important for distinguishing between activities with similar short-term characteristics that differ over a longer period. For example, it is difficult to discriminate between walking around the home and walking away from the home in a data window of 1 s.

4) Downsampling: The data were captured at a sampling rate of 100 Hz and subsequently downsampled to 10 Hz. This was done due to the ESP32 microcontroller's memory and computing power limitations, which we used in our embedded system for experimental purposes.

5) Evaluation of Selected Features: The features, including mean, STD, median, kurtosis, and rms, among others, were extracted from 5-s windows of inertial sensor data (acceleration vector magnitude and gyroscope X, Y, and Z signals) using standard statistical definitions to characterize motion dynamics. Time-domain features like mean, STD, rms, and kurtosis capture motion intensity and irregularity, with rms quantifying overall movement magnitude and kurtosis highlighting deviations from normal walking, both critical for distinguishing "walking away" from home-based activities. In addition, frequency-domain features such as entropy, energy, and skewness were included to characterize dynamic patterns.

Furthermore, computing statistical features over each time window helps reduce accelerometer and gyroscope measurement errors. By summarizing the signal in 5-s windows (e.g., through mean, rms, STD, and entropy), transient spikes or drift in the raw sensor data are effectively averaged out. This means that brief noise bursts or bias in the IMU readings have less influence on the feature values, resulting in more reliable inputs for the classifier.

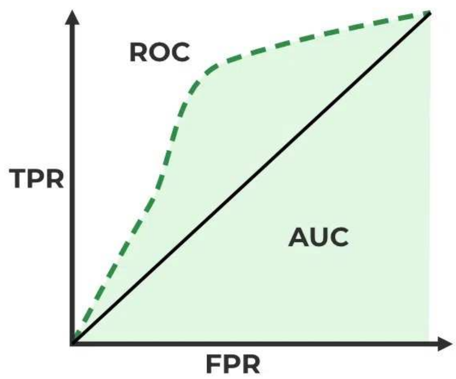

Fig. 4. ROC curve showing the TPR versus FPR, with AUC as an indicator of model performance [60].

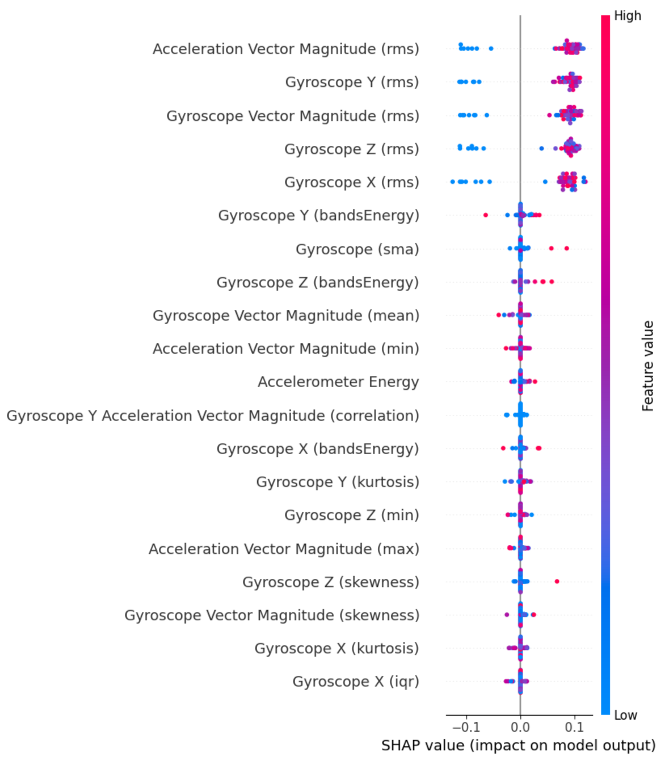

Fig. 5. Feature impact on the XGBoost model output using SHAP.

These features are not manually weighted; instead, they are provided as part of the input feature matrix to the XGBoost algorithm. XGBoost inherently determines their importance through its gradient boosting framework, where features are weighted implicitly based on their contribution to reducing the classification loss during tree construction. The SHAP analysis further elucidates their impact, refining the set to the top ten most discriminative features, as detailed in [42] and [43], thereby reducing overfitting and computational load. This approach ensures the model leverages the most discriminative features without requiring manual weighting, aligning with the computational constraints of our target embedded system.

C. Feature Engineering

In general, feature extraction corresponds to a data transformation process performed on the segmented data. In the context of inertial sensors, this process is necessary because the raw data are not suitable for use by conventional ML algorithms [44].

This study extracted time and frequency domain statistical features on a per-time window basis for the magnitude signals and each axis of the tri-axial accelerometer and gyroscope. Time domain features, such as mean, STD (σ), max, min, angle, meanFreq, rms, median, variance, kurtosis, interquartile range (irq), signal magnitude area (sma), and mean absolute deviation (mad); and frequency domain features, such as entropy (E), bandsEnergy, maxInds, skewness, and energy (ε), among others, were investigated in this study. These features were chosen for their proven effectiveness in characterizing human motion patterns such as movement intensity [28], [29]. Most of the features are well-known statistics and are standard in HAR research. All statistical features (STD, median, kurtosis, and rms) were computed over fixed-length overlapping windows of sensor data (5-s window with 50% overlap). Table I contains the definitions of some of them.

D. Classification Model Selection

The aim of this work is to validate the hypothesis that detecting "moving away from home" is a suitable method for activating GNSS in resource-constrained environments. For this, we need a good classification model, but our goal is not to find the best possible model, but to make a first proof of concept. Therefore, in this section, we will consider four common models in the field of HAR [45], [46], [47], [48], evaluate them, and select the best one.

1) Classification Models: In this section, we briefly describe the classification models used in this study: RF, SVM, LSTM, and XGBoost.

RF generates an ensemble of multiple decision trees to achieve a single, more accurate prediction or result. It is a versatile and computationally efficient algorithm capable of processing large datasets rapidly, is easily adaptable to various ad hoc learning tasks, and returns measures of variable importance [49]. RF is widely used for classification tasks, including the classification of human activities [50].

XGBoost, like RF, is an ensemble learning algorithm based on decision trees, but they have significant differences in how they build and use these trees. XGBoost develops one tree at a time, correcting faults caused by previously trained trees, in contrast to RF, where each tree is generated independently, and the results are aggregated at the end. Trees are planted until none remain [51]. The model uses a gradient descent algorithm to minimize the loss when adding new models. This sequential addition of weak learners (trees) ensures that the shortcomings of previous trees are corrected [52].

SVM is based on mapping datasets to higher dimensions, making it easier to separate data points. By adding higher dimensions, kernel functions simplify the boundaries for nonlinear problems, facilitating the separation of complex data points [53]. SVM has emerged as a potent pattern recognition

TABLE I

SOME OF THE STATISTICAL FEATURES SELECTED. P IS THE PROBABILITY OF AN OCCURRENCE OF EACH OF THE VALUES IN x_i, AND S REPRESENTS THE SIGNAL COMPONENTS ALONG THE x-, y-, AND z-AXIS

Feature	Equation	Feature	Equation
Standard deviation	$\sigma = \sqrt{\frac{1}{N-1}\sum_{i=1}^{N}(x_i - \bar{x})^2}$	Energy	$\varepsilon = \sum_{i=1}^{N} \lvert x_i \rvert^2$
Median	$\mathrm{M} = \left(\frac{\frac{n}{2} - cf}{f}(\omega) + L_m\right)$	sma	$\mathrm{sma}_{xyz} = \frac{1}{3}\left(\sum_{j=1}^{N}\lvert S_{xi}\rvert + \sum_{j=1}^{N}\lvert S_{yi}\rvert + \sum_{j=1}^{N}\lvert S_{zi}\rvert\right)$
Kurtosis	$\mathrm{KV} = \frac{1}{n}\sum_{i=1}^{n}\left(\frac{x_i - \bar{x}}{\sigma}\right)^4$	Skewness	$\mathrm{SV} = \frac{1}{n}\sum_{i=1}^{n}\left(\frac{x_i - \bar{x}}{\sigma}\right)^3$
RMS	$\mathrm{RMS} = \sqrt{\frac{1}{N}\sum_{i=1}^{N} x_i^2}$	Entropy	$\mathrm{E} = \sum_{i=1}^{n} P(x_i)\log_2 P(x_i) P(x_i) = \frac{x_i}{n\sum_{j=1}^{n} x_j}$

tool over the past decade and has been applied to HAR problems [54], [55].

LSTM is a type of deep learning sequential neural network designed to allow information to persist over time. LSTMs excel in processing and analyzing sequential data types like time series, text, and speech. These properties make LSTM outperform traditional ML methods in recognizing various user activities [56].

2) Model Selection Procedure: The procedure for selecting a classification model involved first evaluating the four models using all features. Then, they were evaluated using only the ten features that contributed the most to each model, as determined by the SHAP [57] method. Based on the results of both evaluations, a classification model was selected and then implemented in the embedded system. This two-step evaluation process ensures that the chosen model is both accurate and efficient for real-world applications.

3) Implementation and Training: We implemented the four models using Python-based learning frameworks, specifically, TensorFlow and Scikit-learn. TensorFlow and Scikit-learn are two of the most widely used Python libraries for ML [58]. Scikit-Learn is best suited for traditional ML tasks, offering simplicity and a wide range of algorithms. On the other hand, TensorFlow excels in deep learning, providing scalability, flexibility, and tools for deploying production-ready models [59].

Two elderly participants were recorded for ten days, each for 40 min per day (20 min at home and 20 min walking away from home) at a sampling rate of 10 Hz, resulting in approximately 480 000 samples for each of the six signals (accelerometer x, y, and z, and gyroscope x, y, and z). We then computed the magnitude of both the accelerometer and gyroscope across the x-, y-, and z-axes, creating eight total signals of 480 000 samples each. From these, we selected five signals for further analysis: acceleration vector magnitude, gyroscope vector magnitude, and gyroscope X, Y, and Z. The individual x, y, and z signals of the accelerometer were excluded because their contributions are largely represented in the acceleration vector magnitude. The vector magnitude of acceleration captures the overall movement intensity while reducing computational complexity by simplifying the data into a single scalar value. The gyroscope X, Y, and Z signals were selected to preserve detailed rotational information. Angular velocity, particularly along individual axes, can help differentiate between subtle variations in activities, such as changing direction. A 5-s window was used to generate records, resulting in approximately 9600 records of five signals. For each signal, 17 features were computed, creating a dataset of around 9600 records with 85 features/record.

TABLE II

CONFUSION MATRIX

	Actually Positive (1)	Actually Negative (0)
Predicted Positive (1)	True Positives TPs)	False Positives (FPs)
Predicted Negative (0)	False Negatives (FNs)	True Negatives (TNs)

During the evaluation, 80% of the data was used for training and 20% for testing. The 80–20 split is a well-established practice that ensures a balance between having enough data to effectively train the model and using a sufficient portion for testing to assess the model's generalization capabilities.

Several standard evaluation metrics were used in our experiments to measure our models' performance, including precision, recall, and $F1$-score [32]. These were derived from

TABLE III

PERFORMANCE COMPARISON OF DIFFERENT MODELS ON THE WHOLE FEATURE SET

	Metrics	SVM	XGBoost	RF	LSTM
On the whole feature set	Precision	0.85	0.96	0.92	0.98
	Recall	0.84	0.94	0.91	0.96
	F1-score	0.85	0.95	0.92	0.98
	Accuracy	0.84	0.96	0.91	0.97
	AUC	0.85	0.97	0.93	0.96

TABLE IV

PERFORMANCE COMPARISON OF DIFFERENT MODELS ON SELECTED

	Metrics	SVM	XGBoost	RF	LSTM
On selected features	Precision	0.87	0.98	0.92	0.98
	Recall	0.86	0.97	0.92	0.97
	F1-score	0.85	0.97	0.93	0.98
	Accuracy	0.85	0.97	0.93	0.98
	AUC	0.88	0.97	0.97	0.98

the confusion matrix (see Table II) and applied to the classifier evaluation, as shown in (3)–(5).

Precision is a measure of the accuracy of positive predictions by the ML algorithm, and it is given by

$$\text{Precision} = \frac{\text{TP}}{\text{TP} + \text{FP}}. \tag{3}$$

Recall measures the proportion of actual positive cases that are correctly identified by the algorithm. It is given by

$$\text{Recall} = \frac{\text{TP}}{\text{TP} + \text{FN}}. \tag{4}$$

$F1$-score is the harmonic mean of precision and recall, a more informative model performance evaluation metric than accuracy, given by

$$F1\text{-score} = 2 \times \frac{\text{Precision} \times \text{Recall}}{\text{Precision} + \text{Recall}}. \tag{5}$$

We also computed the overall accuracy scores for the models, a metric that measures how often an ML model correctly predicts the outcome given by

$$\text{Accuracy} = \frac{\text{TP} + \text{TN}}{\text{TP} + \text{TN} + \text{FP} + \text{FN}}. \tag{6}$$

In addition, the area under the receiver operating characteristic (ROC) curve was measured. This metric is widely regarded as the standard for comparing performance. The ROC curve illustrates the optimal decision boundaries by plotting the true positive rate (TPR) against the false positive rate (FPR), as defined by

$$\text{TPR} = \frac{\text{TP}}{\text{TP+FN}} \tag{7}$$

$$\text{FPR} = \frac{\text{FP}}{\text{FP} + \text{TN}}. \tag{8}$$

As illustrated in Fig. 4, the area under the ROC curve (AUC) is widely used to evaluate classifier performance. The AUC value ranges from 0.0 to 1.0, with 1.0 indicating perfect prediction, 0.5 indicating random prediction, and values below 0.5 considered poor predictions [61].

4) Evaluation Using All the Features: This section presents model performance (classification) results when all 85 features were used, and the performance comparison of different models on the whole feature set is presented in Table III.

LSTM and XGBoost outperform SVM and RF in detecting whether a user is walking away from home. LSTM achieves the highest performance across all metrics, with a precision and recall of 0.98, an $F1$-score and accuracy of 0.98, and an AUC of 0.96. XGBoost follows closely with strong precision (0.96), recall (0.94), and AUC (0.97), highlighting its effectiveness in classifying complex activity patterns. RF shows decent results (0.92 for precision and $F1$-score) but lags behind LSTM and XGBoost. With the lowest performance (accuracy and recall of 0.84), SVM struggles to classify the activities.

Overall, the results demonstrate that models such as LSTM and XGBoost, which are better at handling sequential data and complex relationships [51], [62], are better suited for activity classification tasks in dynamic environments like detecting a user walking away from home. These results were refined through a SHAP feature selection process, which will be discussed in Section III-D5.

5) Classification Performance on the Reduced Feature Set: Datasets are often highly dimensional, containing a large number of features, although the relevancy of each feature for analyzing this data is not always clear [63]. Since not all features contribute equally to activity classification, the type and number of features required to perform a given classification task successfully depend on the discriminatory qualities of the features. By involving fewer features in the classification process, the required computational effort (time) and memory are reduced. This requirement is essential in this study since the best model will be exported to an embedded system with limited memory and processing power to test and evaluate our model in a real/natural environment. Also, including every feature creates multiple dimensions, leading to an overfitting problem [64].

To mitigate overfitting caused by extraneous dimensions, we used SHAP [57], a technique that helps understand how individual features influence a model's output. By leveraging the interpretability of SHAP values, we were able to identify and select the most significant features, potentially reducing the feature space while maintaining or even enhancing model performance. Fig. 5 shows the SHAP analysis conducted on the XGBoost model, illustrating each feature's impact on predictions.

In Fig. 5, red dots represent features that had a significant impact on model output, while blue dots indicate features with less impact. We used SHAP values to identify the ten most important features and retrained all models with this reduced feature set. The results obtained using only the selected features (the first ten features) are presented in Table IV.

To assess the impact of individual features on the model's predictions, we used SHAP analysis on the trained XGBoost model. As shown in Fig. 5, features such as the rms of the acceleration vector magnitude and the gyroscope signals (Y, Z, and X) were the most influential, indicating that motion intensity and consistency were key factors in distinguishing

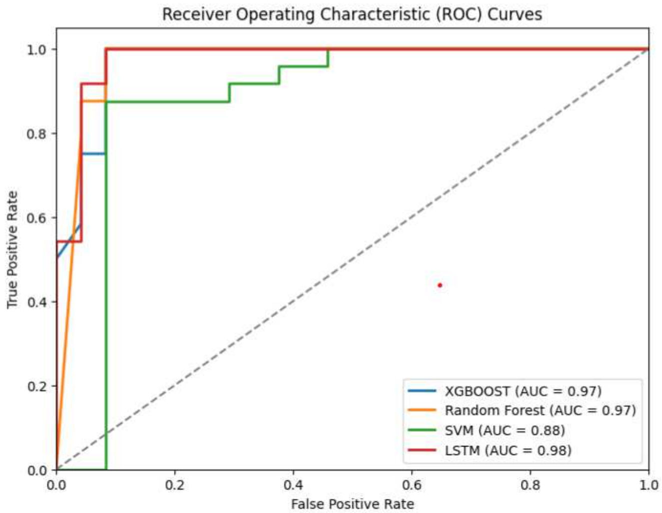

Fig. 6. Results from AUC-ROC.

between the "walking away" and "at home" classes. In addition, band energy from gyroscope signals, especially along the Y- and Z-axes, played a significant role, suggesting that energy in the frequency domain captured periodic motion patterns typical of sustained walking. Other important features included SMA, mean, and kurtosis, which reflected different aspects of variability and irregularity in user movement. Notably, rms-related features dominated the top five most important inputs (contributing approximately 25% to the XGBoost model's predictions), with SHAP values reaching up to ± 0.1, highlighting their central role in the model's decisions. This empirical ranking supports our earlier theoretical explanation (see Section III-B.5) and confirms that the selected time- and frequency-domain features are both statistically meaningful and practically effective in optimizing GNSS activation.

6) Selected Model: In this section, we discuss the results based on selected features applied to the four models used in this experiment.

From the performance on the selected features as shown in Table IV, XGBoost and LSTM demonstrate exceptional accuracy, precision, recall, and $F1$-scores, making them top contenders. In terms of AUC, as illustrated in Fig. 6, the LSTM model delivered the best performance with an AUC of 0.98, showcasing its strong ability to distinguish between "user at home" and "user walking away" activities. Similarly, XGBoost performed exceptionally well with an AUC of 0.97, proving nearly as effective as LSTM in classifying user activities.

XGBoost showed improved performance on the selected features compared to the entire dataset, as evidenced by an increase in precision (from 0.96 to 0.98) and recall (from 0.94 to 0.97), maintaining high AUC values of 0.97 in both cases, as shown in Tables III and IV. LSTM also demonstrated an improvement in AUC, increasing from 0.96 to 0.98, indicating its robustness and enhanced ability to handle feature selection, further emphasizing the strength of both models in managing complex datasets effectively.

Nonetheless, considering the resource-constrained miniature device in which the selected model will be deployed,

TABLE V

COMPARISON OF MODEL SPACE, TRAINING TIME, AND INFERENCE TIME

Model	Space with selected features (MB)	Space with all features (MB)	Training time (ms)	Inference time (ms)
LSTM	1.10	9.3	39711	5086
XGBoost	0.8	6.8	320.8	9.26
SVM	0.7	5.95	65.1	7.8
RF	0.6	5.1	877.6	43.25

factors such as computational efficiency, memory usage, and inference time are paramount. LSTM, though highly accurate, is computationally expensive, requiring significant memory and processing power due to its recurrent nature, which involves storing and processing sequential data over multiple time steps [65]. This makes it less ideal for low-resource environments/devices, where lightweight and energy-efficient models are essential.

XGBoost, on the other hand, strikes a balance between high performance and efficiency. It employs gradient boosting, which is computationally faster than LSTM and more scalable in terms of memory usage. Moreover, XGBoost can be optimized through early stopping and parallelization, further enhancing its suitability for deployment in resource-constrained settings [33], [52]. XGBoost's ability to manage nonlinear relationships without the same resource demands as LSTM gives it a clear advantage in environments with limited processing power and memory.

SVM lags behind in overall performance, indicating limited generalization of unseen data. This is likely due to their linear nature, which may not effectively capture the complexity of the dataset. Its performance is adequate but may not be ideal for large-scale or complex environments where high accuracy and recall are critical, as in this study. In contrast, despite promising results on the selected features, RF still falls slightly behind XGBoost in accuracy (0.93) and AUC (0.93), possibly due to its lack of boosting, which limits its ability to reduce bias. However, it may still be viable in scenarios where computational constraints are strict but performance requirements are moderate.

It should be noted that all the models performed better on selected features than on the whole feature set, highlighting the importance of feature reduction in our work. Their performances are also demonstrated in Fig. 7, with all models easily differentiating home activities from walking away from home, a key feature in GNSS activation. Fig. 8 shows the $F1$-scores for different models on selected features against the whole dataset. LSTM [see Fig. 7(d)] performs best with minimal misclassifications (18 false positives and 34 false negatives), indicating superior accuracy in activity differentiation.

Considering the resource-constrained miniature device in which the selected model will be deployed, factors such as computational efficiency, memory usage, and inference time are of high importance. LSTM, while offering strong accuracy, requires considerable computational power and memory, as illustrated in Table V. Table V presents the comparison of models in terms of memory space, training, and inference times. This makes LSTM less practical for low-resource

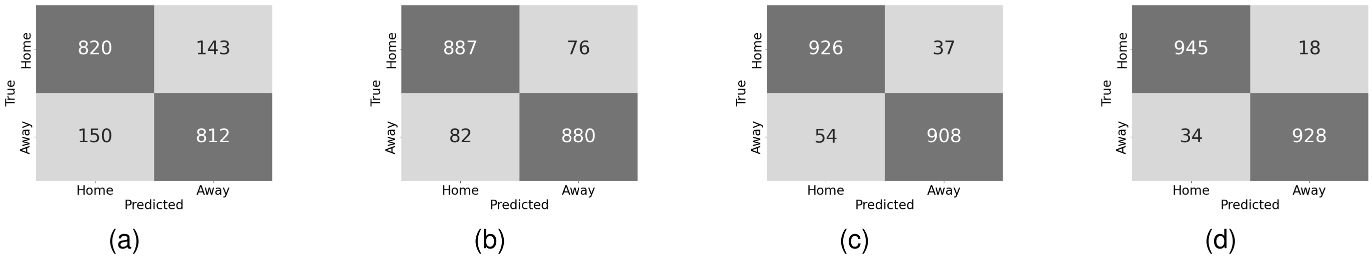

Fig. 7. Confusion matrix for all models using only selected features. Home: "at home"; Away: "walking away." (a) Confusion matrix SVM model. (b) Confusion matrix for the RF model. (c) Confusion matrix for the XGBoost model. (d) Confusion matrix for LSTM model.

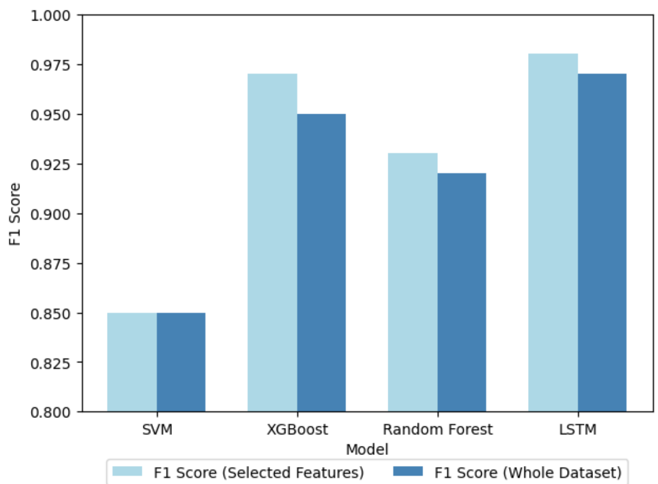

Fig. 8. $F1$-scores for different models on selected features versus the whole dataset.

devices. XGBoost, in contrast, provides a balance between performance and efficiency, with lower computational and memory space demands compared to LSTM, making it more appropriate for resource-constrained environments.

In conclusion, the tradeoffs between performance and resource efficiency make XGBoost the most suitable model for deployment in resource-limited environments. Its high accuracy and AUC scores, coupled with its computational efficiency, make it the ideal model to export to our low-cost resources device.

IV. GNSS Activation Tests

The goal of the experiments is to practically use our ML model embedded on the device to assist in distinguishing or reporting whether a user is around home or moving away from home, with the purpose of triggering GNSS activation or not.

In these experiments, we demonstrate that relying solely on user motion or acceleration to turn on the GNSS is insufficient, particularly with human participants. This work presents a more efficient and smarter algorithm for GNSS activation that employs ML to differentiate between users' activities or motion modes while at home versus those moving away from home, as demonstrated in our experiments.

A. Experiments Description

We carried out various experiments to evaluate the effectiveness of our developed method, specifically focusing on GNSS activation and the impact of user activity classification. To assess our GNSS activation approach, we compared it with a method we implemented, which was inspired by existing literature [24]. This system triggers the GPS based on the user's mobility state, turning it on when the user is in motion and deactivating it once stationary for a configurable interval of 10 min. The following three experiments were used to evaluate our system as follows.

1) *Experiment One: Continuously Walking at Home:* In this experiment, the user continuously walks (in motion) inside the house from one room to another and around the home for 6 min. The aim of this experiment is to illustrate that in our approach, the GNSS is not activated solely when walking within and around the home, despite both activities involving walking. Hence, there is power saving compared to the user motion-based method, where the GNSS will continuously be active as the user's mobility state is constantly in an in-motion state.
2) *Experiment Two: Everyday User Activities at Home:* In this experiment, we conducted daily user activities within and around the home, and as the user walked away from home to work. The activities included walking from one room to another, sitting, sleeping, standing, washing utensils, and finally, walking away from home. Each of these six activities lasted 2 min. The goal of this experiment is to demonstrate that our approach does not mistake any home activities for walking away from home activities.
3) *Experiment Three: Walking at Home Against Walking Away:* Walking (in motion) continuously inside the house from one room to another, around the home for 6 min, and after walking away from home, also for 6 min. This experiment aims to demonstrate that the GNSS is only activated when the user "walks away" from home. It also shows that our model easily distinguishes walking around the home from walking away from home.

B. Model Integration and Hardware Setup

1) Model Deployment and Data Collection: LSTM was the best model, but could not be installed in our embedded system because of the memory and computation power limitations (see

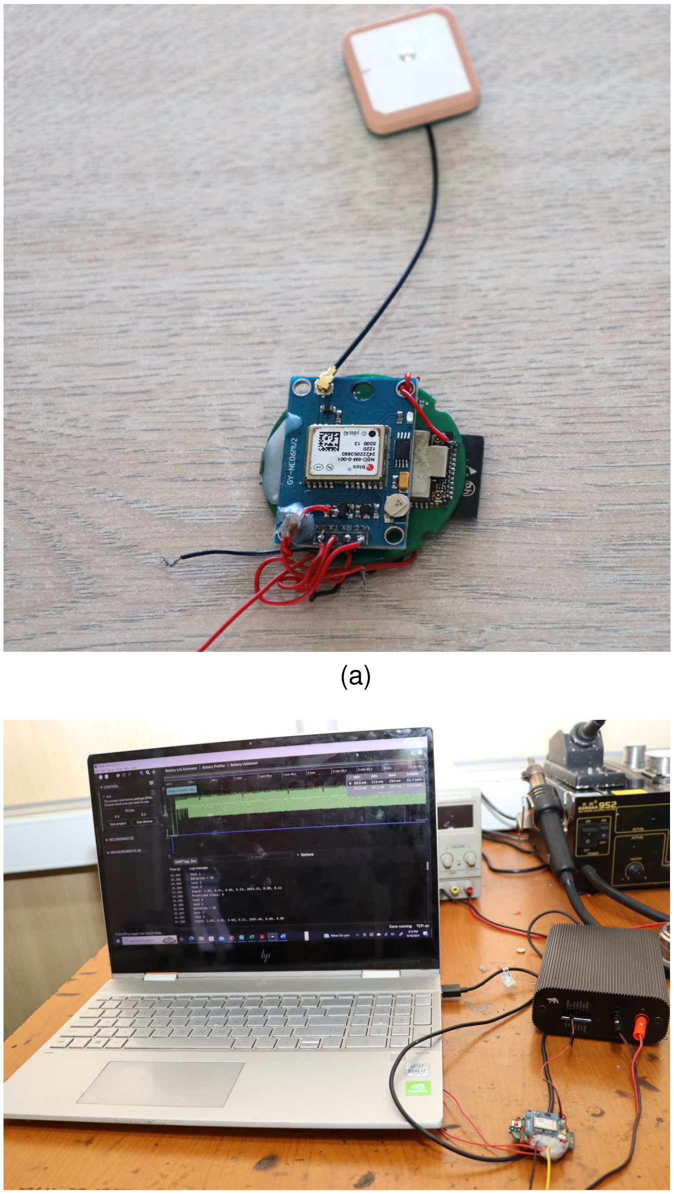

(a)

(b)

Fig. 9. Designed embedded system. (a) PCB. (b) Experimental setup.

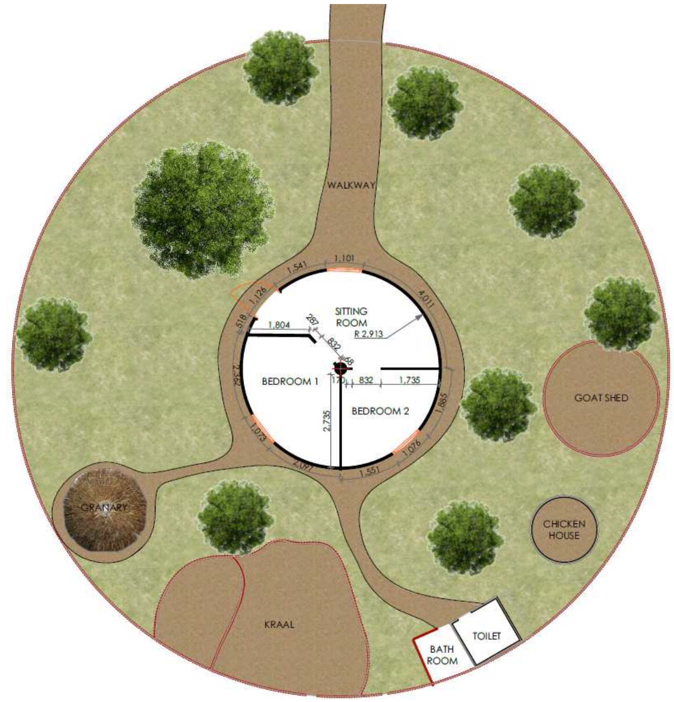

Fig. 10. House plan simulated to conduct the three experiments.

Table V) even after feature reduction. Therefore, the second-best model, XGBoost, was selected and used in experiments. The selected XGBoost model was converted to a lightweight model and deployed on our designed embedded system using Eloquent ML libraries, which port the model to C++ code that runs on the ESP32 microcontroller.

For this experiment, an embedded system was developed and assembled on a custom-designed printed circuit board (PCB), as illustrated in Fig. 9(a). The PCB integrates an ESP32 microcontroller (with a sleep current of less than 5 μA, ideal for battery-powered wearables), a six-axis IMU (MPU6050), and a NEO6 GPS module for positioning. The GPS module's compact architecture and power efficiency make it suitable for battery-powered devices that face space and cost limitations. In addition, it includes a small battery for hot starts and has a built-in EEPROM to store configuration settings when powered off. The PCB also facilitates lithium-ion battery charging through an onboard USB connector, allowing for easy programming. This custom design allowed for system miniaturization, making it suitable to be worn or carried by the user.

We also used the Otii Arc Pro, a high-precision energy consumption analysis tool, to measure the power consumption of our system [66]. Otii Arc Pro and our embedded system communicated via USART serial interface, with a baud rate of 115 200, to capture logs for analysis, as shown in Fig. 9(b). GNSS data are not used as input features for the machine learning model. Instead, we activate the GNSS receiver after classification for location tracking. Each activation measures the GNSS module's power consumption (via Otii Arc Pro), allowing us to quantify battery savings compared to always-on or motion-based activation methods.

2) Experiment Execution: We carried out our experiments in an open field at Makerere University, Kampala football ground, aiming to replicate a resource-constrained rural environment characterized by semi-structured, scattered, poorly constructed buildings and minimal GNSS signal disruption. To simulate the home setup accurately, we recreated the house plan depicted in Fig. 10 by using cones to demarcate key sections and boundaries. Using cones allowed us to represent important areas of the house in an open environment, thus providing a realistic yet controlled setting. During the data collection phase, the participant (volunteer) attached the embedded device to their wrist and carried out the experiments as outlined in Section IV-A.

We automatically record the raw inputs of the accelerometer and gyroscope at a sampling rate of 10 Hz. These are then windowed using a window size of 5 s, and each of the top ten selected features is computed across each window. These

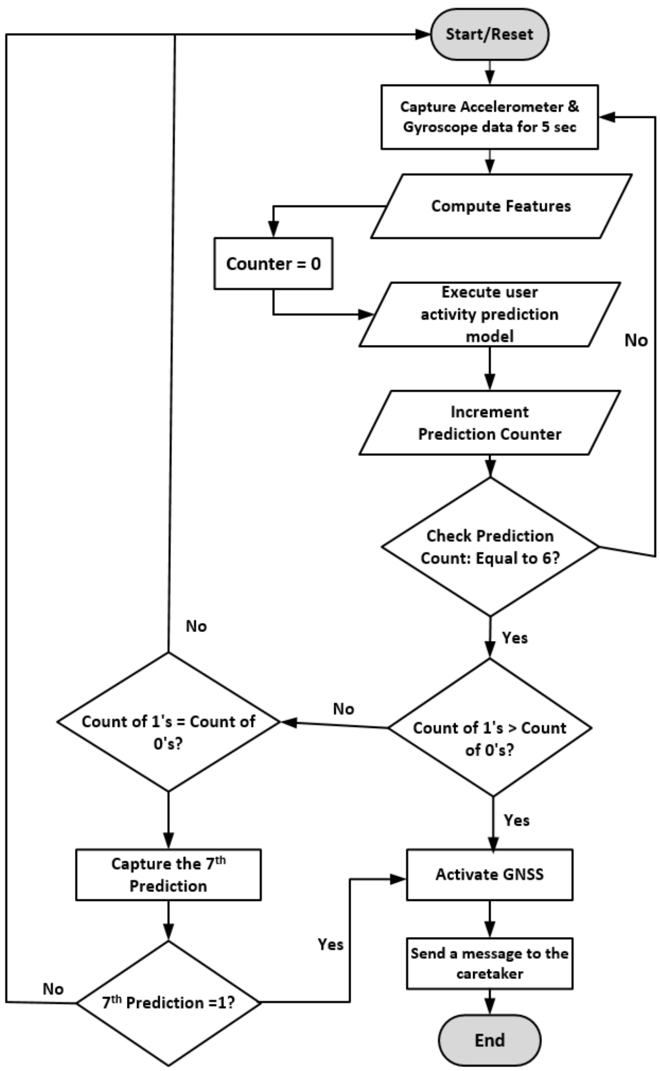

Fig. 11. Flowchart for our user activity-based GNSS activation system.

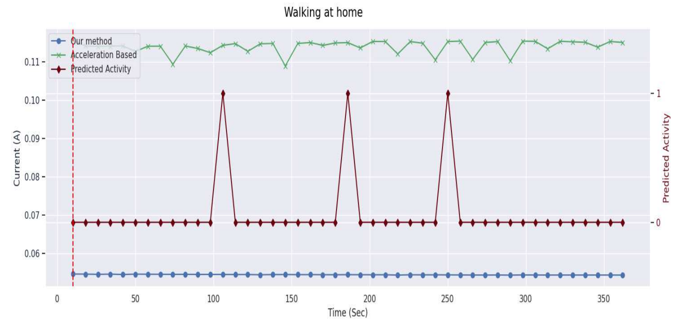

Fig. 12. Power consumption of the proposed model versus the motion-based method as the user continuously moves around at home. 0: "at home"; 1: "walking away."

are then sent into the ported model to obtain a prediction of whether the person with the device is "walking away" or "at home."

3) GNSS Activation: Our system only activates the GNSS when the user activity is presumed to be walking away based on a sequence of predictions as illustrated in Fig. 11. Our system is designed to determine whether a user is around the home (prediction class 0) or walking away (prediction class 1). Depending on the output, the counter is updated at the end of every prediction. After six predictions, the system evaluates the results; if prediction class 1 outnumbers class 0, the system activates GNSS and notifies the caretaker. The decision to use six predictions aims to balance safety with system efficiency; 30 s is a good enough time to respond, considering this system is designed to monitor elderly people; their safety is paramount, and timely responsiveness is essential. Evaluating six predictions ensures quick and reliable action while avoiding unnecessary GNSS activation. A seventh prediction determines the final action in cases of an even split. If this prediction indicates class 1, GNSS is activated, and a notification is sent. This approach ensures GNSS activation only when there's a clear indication of the user leaving home, minimizing unnecessary activation and alerts.

C. Results and Discussion

The results and analysis of the three experiments that were conducted are presented in Sections IV-C1–IV-C3.

1) Experiment One: Continuously Walking at Home: In experiment one, the user walked continuously for 6 min, moving between rooms and around the home. This setup aimed to evaluate the classifier's performance and power consumption during sustained user movement.

Fig. 12 presents the results of both the classification model and the power consumption analysis for this activity. The classifier's output and power usage for our proposed method are compared with the acceleration-based model, highlighting the performance differences in terms of GNSS activation and energy efficiency.

The classification results demonstrate that our method accurately identified most of the "walking at home" activities as "at home," ensuring that GNSS was not activated during the 6-min continuous walk. Although there were three instances where the activity was misclassified as "walking away," the final decision logic of our system (detailed in Fig. 11) was designed to disregard these outliers, preventing unnecessary GNSS activation.

In terms of GNSS activation and power consumption, our method maintained a much lower and stable current draw, around 0.055 A, compared to the acceleration-based method, which exhibited higher consumption, fluctuating between 0.10 A and 0.12 A throughout the experiment. It should be noted that in resource-constrained rural environments, people spend most of their time outdoors around their houses, so it is unnecessary to activate the GNSS so frequently to monitor them. Results show that our model does not classify walking at home as walking away, in contrast to a basic walk detector. This helps to avoid enabling GNSS when the user is around the same location, saving some energy.

For example, with a 4000-mAh battery, the acceleration-based model would last approximately 1.5 days, as shown in Fig. 13 from the Otii battery estimator. Our method extends the battery life to 3.1 days, resulting in over 40% battery savings. This demonstrates the superior efficiency of our model

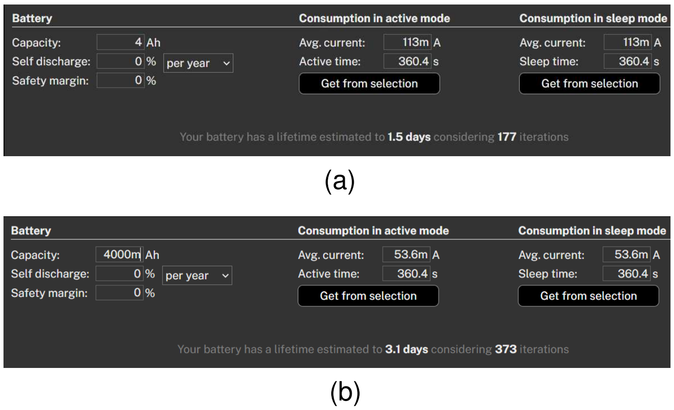

Fig. 13. Battery life estimation for our method against the motion-based during experiment one. (a) Battery life estimation with the acceleration-based method. (b) Battery life estimation with our method.

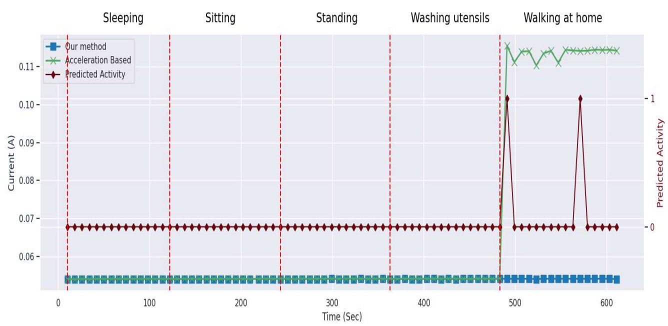

Fig. 14. Performance of our model versus the motion-based method during everyday user activities within and around the home during experiment 2. 0: "at home"; 1: "walking away."

and highlights its suitability for continuous activity monitoring around the home, particularly in resource-constrained environments.

2) Experiment Two: Everyday User Activities at Home: Fig. 14 presents the analysis of the gathered data during experiment two, in which the user walked without interruption (continuously) for 6 min from one room to another and around the home, followed by an additional 6 min of walking away from the home. The figure illustrates both the classification results and power consumption analysis for our proposed model against an acceleration-based model.

Our model correctly classified most activities within the home, ensuring that the GNSS was never activated during these activities. The classification results show that activities such as sitting, standing, sleeping, and washing utensils were correctly predicted as "at home" without unnecessary GNSS activation.

Regarding power consumption, both models showed minimal current usage during stationary activities like sitting, standing, sleeping, and washing utensils, with consumption at approximately 0.055 A. However, during the "walking at home" activity, the acceleration-based method's power consumption increased significantly, with current spikes ranging between 0.1 and 0.12 A, due to unnecessary GNSS activation triggered by motion detection. In contrast, our method maintained a stable low consumption of around 0.055 A

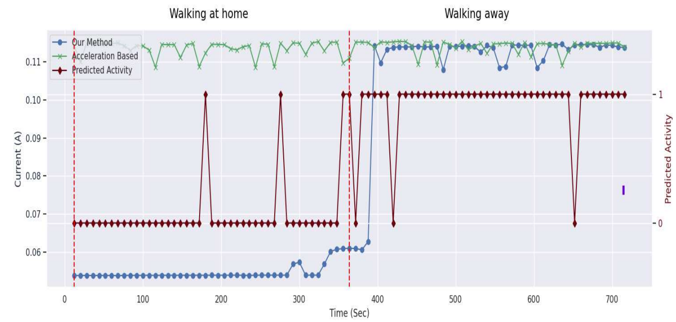

Fig. 15. Power consumption of the motion-based method against our model as the user walks around the home and away from home during experiment 3. 0: "at home"; 1: "walking away."

throughout, showcasing better power efficiency. Despite some false classifications of "walking away" during the "walking at home" activity, our method was robust enough to avoid GNSS activation, as it effectively ignored these outliers based on the decision-making flow outlined in Fig. 11. It should be noted that the red vertical delimiters represent the activity ground truth.

3) Experiment Three: Walking at Home Versus Walking Away: Fig. 15 presents the analysis of the gathered data during experiment three, in which the user walked without interruption (continuously) from one room to another and around the home, followed by walking away from the home. The figure illustrates both the classification results and power consumption analysis for our proposed method and the acceleration-based method. The red vertical delimiters represent the activity ground truth, providing a reference for model performance.

Our model effectively classified most home activities without activating GNSS during the continuous walk around the home. Unlike the acceleration-based model, which kept GNSS active and showed increased power consumption (0.1–0.12 A), our model consistently maintained a low consumption of around 0.055 A and only activated GNSS when the user walked away.

The results, even though on short-duration activities, demonstrate that our model offers significant power efficiency advantages over the acceleration-based approach by consuming minimal power when the user remains at home and only increasing consumption when necessary. Moreover, accurate activity predictions ensured energy use aligned with real-time user actions, making our model a more sustainable solution for continuous monitoring applications, especially for tracking elderly individuals with dementia in resource-constrained environments.

The conducted experiments provided power consumption data based on short-duration activities, and so to better illustrate real-world savings, we extrapolated these findings to a realistic daily scenario typical of elderly individuals in rural, resource-constrained settings. Given that elderly people generally spend most of their day (approximately 10–12 h) at home or within close proximity performing routine, low-intensity activities, and roughly 1 hour daily actively walking away from home for tasks like fetching water or visiting

TABLE VI
SUMMARY AND COMPARISON OF EXPERIMENTAL RESULTS

Experiment	Method	GNSS Activation Frequency	Battery Life (4000 mAh battery)	Battery Saving (%)
Continuously walking at home (6 min)	Acceleration-based	Continuous activation	1.5 days	Baseline (0%)
	Our method	No activation	**3.1 days**	**>40%**
Everyday activities (12 min total)	Acceleration-based	Frequent activation	1.8 days	Baseline (0%)
	Our method	Minimal activation (only when leaving home)	**3.2 days**	**>40%**
Walking at home vs. walking away (12 min)	Acceleration-based	Activated during both	1.6 days	Baseline (0%)
	Our method	Activated only when "walking away"	**3.0 days**	**>40%**

nearby neighbors or trading centers, our GNSS activation method, which specifically detects the "walking away" activity class, can significantly reduce unnecessary activations.

Using our experimental data indicating a 40% reduction in power consumption compared to conventional activity-based GNSS activation methods, we estimate that with a standard 4000-mAh battery, the frequency of required recharging could reduce from approximately once every two days (typical for motion-based methods) to about once every four to five days. This extended battery life significantly reduces the burden on elderly users or their caregivers, who often must travel considerable distances—typically several kilometers—to trading centers for battery recharging. Thus, our approach not only extends battery life but substantially improves the practicality and sustainability of remote monitoring solutions in resource-constrained environments.

To provide a clear comparative overview of the results and better illustrate the performance of our proposed model relative to existing methods, Table VI summarizes the GNSS activation frequencies, estimated battery life, and energy savings across all conducted experiments.

From Table VI, it is clear that our method consistently provides over 40% energy savings compared to generic motion-based GNSS activation methods. These results support our hypothesis that explicitly detecting "walking away" significantly reduces unnecessary GNSS activations and improves battery performance, aligning with the specific needs of remote elderly monitoring in resource-constrained settings.

D. Model Validation on Public Datasets

To assess the model's generalizability beyond the initial study involving two elderly participants, we evaluated the trained XGBoost model on three public human activity datasets. This validation demonstrates the method's ability to maintain high performance across diverse cohorts and activities, reducing the risk of overfitting. By utilizing external datasets with larger and more varied subject groups, we highlight the model's robustness and applicability to broader populations.

1) Datasets: We utilized three publicly available datasets to assess the generalizability of our GNSS activation approach beyond our collected data as follows.

a) IPIN2017 public dataset: Collected as part of a study [67] evaluating wearable INS in large indoor and outdoor environments, this dataset includes inertial measurements from IMUs mounted on the foot, wrist, thigh (in pocket), and glasses, captured during pedestrian walks across a 14 380 m^2 area. It contains data from six subjects, identified by dates (e.g., March 23, 2017), with over 69 georeferenced ground truth points for accurate positioning. In line with our wrist-worn training setup, we only kept the wrist-mounted recordings, similar to a smartwatch on a low-movement arm, and excluded data from the foot, thigh, and glasses. This maintained methodological consistency for the elderly-monitoring use case examined in this study, particularly aligning with the "walking away" scenario.

b) UCI HAR dataset: This dataset includes inertial data from 30 volunteers (aged 19–48 years) performing six activities of daily living (ADLs): walking, walking downstairs, walking upstairs, laying, standing, and sitting. It is publicly available through the UCI ML repository [68]. All signals were recorded using a Samsung Galaxy S II smartphone (triaxial accelerometer and gyroscope, 50 Hz) firmly strapped to the waist, that is, rigidly attached to the trunk. This trunk-mounted setup is motion-wise equivalent to the wrist-worn configuration used during our data collection (and later for training the model), supporting the use of UCI HAR for generalization analysis. The inclusion of a broader age range and larger sample size than in our original study further enhances the dataset's value for evaluating model generalization. This dataset provides additional evidence that our model is also effective for a younger age group.

c) GeoTecINIT dataset: Detailed in a 2023 data in brief publication [69], this dataset, collected by the GEOTEC Research Group at the University Jaume I in Castellón de la Plana, Spain, provides inertial measurements from a smartphone (carried in the left trouser pocket) and a smartwatch (worn on the left wrist) for 23 diverse subjects. Participants performed five activities (seated, standing up, walking, turning, and sitting down) aligned with the timed up and go (TUG) test, which was recorded at approximately 100 Hz, yielding over 259 000 smartphone samples and 262 000 smartwatch samples. Available on Zenodo [70]. To maintain consistency with our wrist-worn training setup, we only consider smartwatch recordings that match the low-arm-movement wrist configuration used for elderly monitoring and exclude pocket-carried smartphone data. The dataset's broader age range, gender balance, and inclusion of dynamic postural transitions offer an additional test bed for assessing the model's adaptability.

2) Experimental Setup: To address the concern about generalization, we applied the same ten-feature windowed preprocessing pipeline (5-s windows, 50% overlap, 10 Hz) described in Section III-C to all datasets, ensuring consistency with the original training process. The XGBoost model, trained solely on data from the two original participants, was used without retraining to classify activities as "Home" or "Away." This no-retraining approach tests the model's ability to

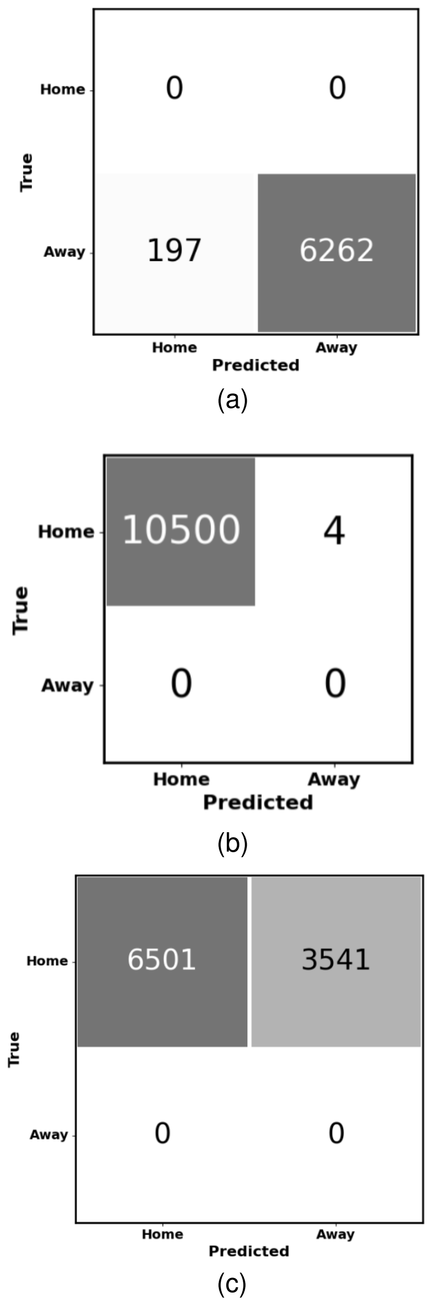

Fig. 16. Confusion matrices for the XGBoost model on the three public datasets. Home: "at home"; Away: "walking away." (a) Confusion matrix for the IPIN2017 dataset. (b) Confusion matrix for the UCI HAR dataset. (c) Confusion matrix for GeoTecINIT dataset.

generalize to unseen data, directly addressing the risk of overfitting. Performance was evaluated using confusion matrices and standard metrics: accuracy, precision, recall, and $F1$-score. Due to the lack of explicit "Home" or "Away" labels, we assigned labels based on activity context: all walking activities in IPIN2017 were labeled "Away" (aligned with long outdoor walks), while all activities in UCI HAR and GeoTecINIT were labeled "Home" (reflecting indoor daily living or transitional activities).

3) Results: Table VII summarizes the classifier's performance across the datasets. On the IPIN2017 dataset, the model

TABLE VII
CROSS-DATASET EVALUATION OF OUR CLASSIFIER ON THREE PUBLIC DATASETS

Dataset	#Windows	Accuracy	Precision	Recall	F1 Score
IPIN2017	6 459	0.97	1.00	0.97	0.98
UCI HAR	10 504	1.00	1.00	1.00	1.00
GeoTecINIT	10 042	0.65	1.00	0.65	0.79

achieved 96.95% accuracy, misclassifying only 197 out of 6459 windows as "Home." For the UCI HAR dataset, which includes various ADLs from 30 subjects, the model attained 99.95% accuracy, correctly classifying 10 500 out of 10 504 windows. In contrast, the GeoTecINIT dataset, featuring transitional activities from 23 subjects, posed a challenge, yielding 64.74% accuracy. The high performance on IPIN2017 and UCI HAR suggests effective handling of "Away" and typical "Home" activities, respectively. The lower accuracy on GeoTecINIT, likely due to differences in activity types (TUG test versus daily living), indicates potential limitations in adapting to diverse patterns, highlighting the need for further refinement. Fig. 16 presents confusion matrices, which visually depict the error distribution across home/away classes for each dataset.

E. Discussion

Our model has effectively demonstrated its ability to differentiate between user activities "at home" and "walking away," thereby minimizing unnecessary GNSS activation. This approach extends battery life by more than 40% when the user remains around the home. The model has also shown reliability in accurately detecting when a user walks away and activating the GNSS with minimal errors, as validated across multiple tests. While a small number of "walking away" activities were misclassified as "at home," this did not affect the GNSS activation decision, thanks to our decision logic (see Fig. 11). To ensure reliability, we tested the model on public datasets, including IPIN2017, UCI HAR, and GeoTecINIT, achieving accuracies of 96.95%, 99.95%, and 64.74%, respectively. Although we did not collect these datasets ourselves, their inclusion in our evaluation demonstrates that the model's behavior is consistent across different cohorts, activities, and recording conditions, providing strong evidence of generalizability. It is evident that user motion alone is insufficient to justify GNSS activation, as movement does not always indicate danger or a need for caretaker intervention. Activating GNSS solely based on motion would lead to unnecessary energy consumption and reduced battery life, which is especially critical in resource-constrained areas with limited access to electricity.

V. CONCLUSION

This article presents a novel ML-driven GNSS activation method tailored to resource-constrained environments for detecting the activity of walking away from home to another location, with the purpose of triggering (activating or deactivating) the GNSS. The core idea of our proposal is detecting the activity “walking away” from home. We hypothesize this is sufficient for resource-constrained environments, as this approach eliminates the need for beacons, avoids assumptions about varying signal strengths indoors and outdoors, is better than just a basic acceleration signal thresholding, and is simpler than HAR since we don’t need to classify different daily user activities. This approach harnesses the power of ML to discern between user motion modes at home and when moving to a different location.

Our proposed ML-driven GNSS activation method accurately differentiates between home-based and walking-away-from-home activities, minimizing unnecessary GNSS activations while ensuring reliable and timely alerts when users move away from home. This reduces false alarms and optimizes performance for continuous monitoring systems, offering a sustainable and practical solution for real-world applications, particularly for elderly monitoring in resource-constrained settings. A comparative analysis against generic activity-based GNSS activation methods demonstrates significant battery-life improvements of more than 40%, highlighting the targeted approach’s efficacy.

The model’s robustness is further validated through its performance on three public datasets: IPIN2017, UCI HAR, and GeoTecINIT, as detailed in Section IV-D. It achieves high accuracies of 96.95% on IPIN2017 for “Away” activities and 99.95% on UCI HAR for “Home” activities, demonstrating strong generalization across diverse cohorts and varying sensor configurations. However, the lower accuracy of 64.74% on GeoTecINIT indicates challenges with diverse activity patterns and different sensor types, suggesting areas for further refinement. This external validation supports the method’s applicability to broader populations and reassures against overfitting.

In future work, we plan to explore advanced and integrated ML models. We will also plan to improve the accuracy and adaptability of the ML models by incorporating more diverse datasets, including a wider range of user behaviors and environmental conditions. This would enable the system to generalize better across different users and contexts, increasing its robustness.

Acknowledgment

This article reflects only the author’s view, and the Research Executive Agency is not responsible for any use that may be made of the information it contains.

References

[1] D. E. Bloom and L. M. Zucker, “*Aging is the real population bomb*,” Finance Develop., Int. Monetary Fund, Washington, DC, USA, 2023, vol. 60, no. 2.

[2] United Nations, Department of Economic and Social Affairs, Population Division, “World population ageing 2020: Highlights: Living arrangements of older persons,”, United Nations, New York, NY, USA, Tech. Rep. ST/ESA/SER.A/451, 2021.

[3] E. Jaul and J. Barron, “Age-related diseases and clinical and public health implications for the 85 years old and over population,” *Frontiers Public Health*, vol. 5, Dec. 2017, Art. no. 316964.

[4] N. Neubauer, P. Azad-Khaneghah, and L. Liu, “What do we know about strategies to manage dementia-related wandering? A scoping review,” *Gerontechnology*, vol. 17, no. s, p. 170, Apr. 2018.

[5] M. Ratnayake et al., “Aging in place: Are we prepared?,” *Delaware J. Public Health*, vol. 8, no. 3, p. 28, Mar. 2022.

[6] J. Binette and F. Farago, “Where we live, where we age: Trends in home and community preferences,” AARP, Washington, DC, USA, AARP Res. Rep., 2021.

[7] *Towards Long-term Care Systems in Sub-saharan Africa*, World Health Organizatio, Geneva, Switzerland, 2017.

[8] G. V. Angelov, D. P. Nikolakov, I. N. Ruskova, E. E. Gieva, and M. L. Spasova, “Healthcare sensing and monitoring,” in *Enhanced Living Environments: Algorithms, Architectures, Platforms, and Systems*. Cham, Switzerland: Springer, 2019, pp. 226–262.

[9] S. Wang et al., “Technology to support aging in place: Older adults’ perspectives,” in *Healthcare*, vol. 7. MDPI, 2019, p. 60.

[10] S. Kim, K. Z. Gajos, M. M´’uller, and B. J. Grosz, “Acceptance of mobile technology by older adults: A preliminary study,” in *Proc. 18th Int. Conf. Human-Comput. Interact. Mobile Devices Services*, Sep. 2016, pp. 147–157.

[11] M. Jacob Rodrigues, O. Postolache, and F. Cercas, “Physiological and behavior monitoring systems for smart healthcare environments: A review,” *Sensors*, vol. 20, no. 8, p. 2186, Apr. 2020.

[12] A. P. Junior, L. E. Díez, A. Bahillo, and O. S. Eyobu, “Remote pedestrian localization systems for resource-constrained environments: A systematic review,” *IEEE Access*, vol. 11, pp. 36865–36889, 2023.

[13] H. Bernd. (2021). *Low-power Gnss for Tracking Applications*. [Online]. Available: https://content.u-blox.com/sites/default/files/Low-power-tracking-applications_WhitePape_UBX-21014570(1).pdf

[14] C. J. Matz, D. M. Stieb, and O. Brion, “Urban-rural differences in daily time-activity patterns, occupational activity and housing characteristics,” *Environ. Health*, vol. 14, no. 1, pp. 1–11, Dec. 2015.

[15] Z. Dai and F. J. W. Podd, “A power-efficient BLE augmented GNSS approach to site-specific navigation,” in *Proc. IEEE/ION Position, Location Navigat. Symp. (PLANS)*, Apr. 2020, pp. 1305–1310.

[16] L. Zhang, J. Liu, H. Jiang, and Y. Guan, “SensTrack: Energy-efficient location tracking with smartphone sensors,” *IEEE Sensors J.*, vol. 13, no. 10, pp. 3775–3784, Oct. 2013.

[17] S. Abghari, V. Boeva, E. Casalicchio, and P. Exner, “An inductive system monitoring approach for GNSS activation,” in *Proc. IFIP Int. Conf. Artif. Intell. Appl. Innov.*, 2022, pp. 437–449.

[18] Y. Zhu et al., “A fast indoor/outdoor transition detection algorithm based on machine learning,” *Sensors*, vol. 19, no. 4, p. 786, Feb. 2019.

[19] A. P. Junior, L. E. Díez, A. Bahillo, and O. S. Eyobu, “A resource-efficient approach of GNSS activation for pedestrian monitoring,” in *Proc. Mobile Ubiquitous Syst., Comput., Netw. Services*. Cham, Switzerland: Springer, Jul. 2024, pp. 526–546.

[20] C.-M. Huang, C.-H. Lee, and W.-S. Chen, “A power efficient pedestrian touring scheme based on sensor-assisted positioning and prioritized caching for smart mobile devices,” in *Proc. 21st Int. Conf. Softw., Telecommun. Comput. Netw. (SoftCOM)*, Sep. 2013, pp. 1–5.

[21] F. B. Abdesslem, A. Phillips, and T. Henderson, “Less is more: energy-efficient mobile sensing with SenseLess,” in *Proc. 1st ACM Workshop Netw., Syst., Appl. for Mobile Handhelds (MobiHeld)*, Barcelona, Spain, 2009, pp. 61–62.

[22] R. Anacleto, L. Figueiredo, A. Almeida, and P. Nováis, “Person localization using sensor information fusion,” in *Proc. Ambient Intelligence-Software Applications: 5th Int. Symp. Ambient Intell.*, 2014, pp. 53–61.

[23] M. B. Kjærgaard, J. Langdal, T. Godsk, and T. Toftkjær, “EnTracked: Energy-efficient robust position tracking for mobile devices,” in *Proc. 7th Int. Conf. Mobile Syst., Appl., services*, Jun. 2009, pp. 221–234.

[24] T. O. Oshin, S. Poslad, and A. Ma, “Improving the energy-efficiency of GPS based location sensing smartphone applications,” in *Proc. IEEE 11th Int. Conf. Trust, Secur. Privacy Comput. Commun.*, Jun. 2012, pp. 1698–1705.

[25] J. Paek, J. Kim, and R. Govindan, “Energy-efficient rate-adaptive GPS-based positioning for smartphones,” in *Proc. 8th Int. Conf. Mobile Syst., Appl., services*, Jun. 2010, pp. 299–314.

[26] X. Ye, K. Sakurai, N. C. Nair, and K. I. Wang, “Machine learning techniques for sensor-based human activity recognition with data heterogeneity—A review,” *Sensors*, vol. 24, no. 24, p. 7975, Dec. 2024.

[27] M. Webber and R. F. Rojas, “Human activity recognition with accelerometer and gyroscope: A data fusion approach,” *IEEE Sensors J.*, vol. 21, no. 15, pp. 16979–16989, Aug. 2021.

[28] A. Bulling, U. Blanke, and B. Schiele, “A tutorial on human activity recognition using body-worn inertial sensors,” *ACM Comput. Surveys*, vol. 46, no. 3, pp. 1–33, Jan. 2014.

[29] O. D. Lara and M. A. Labrador, "A survey on human activity recognition using wearable sensors," *IEEE Commun. Surveys Tuts.*, vol. 15, no. 3, pp. 1192–1209, 3rd Quart., 2013.
[30] J. Wang, Y. Chen, S. Hao, X. Peng, and L. Hu, "Deep learning for sensor-based activity recognition: A survey," *Pattern Recognit. Lett.*, vol. 119, pp. 3–11, Mar. 2019.
[31] H. F. Nweke, Y. W. Teh, M. A. Al-Garadi, and U. R. Alo, "Deep learning algorithms for human activity recognition using mobile and wearable sensor networks: State of the art and research challenges," *Expert Syst. Appl.*, vol. 105, pp. 233–261, Sep. 2018.
[32] M. Sokolova and G. Lapalme, "A systematic analysis of performance measures for classification tasks," *Inf. Process. Manage.*, vol. 45, no. 4, pp. 427–437, Jul. 2009.
[33] S. Netanel. (2021). *Xgboost Vs Lstm: A Comparative Analysis of Time Series Forecasting for Stock Price Prediction*. Accessed: Aug. 25, 2024. [Online]. Available: https://netanel.io/posts/xgb_vs_lstm/#lstm-long-short-term-memory
[34] A. Esmaeili Kelishomi, A. H. S. Garmabaki, M. Bahaghighat, and J. Dong, "Mobile user indoor-outdoor detection through physical daily activities," *Sensors*, vol. 19, no. 3, p. 511, Jan. 2019.
[35] C. Kelvin. (2024). *Sensor Logger*. [Online]. Available: https://www.tszheichoi.com/sensorlogger
[36] M. J. Mathie, A. C. F. Coster, N. H. Lovell, and B. G. Celler, "Accelerometry: Providing an integrated, practical method for long-term, ambulatory monitoring of human movement," *Physiological Meas.*, vol. 25, no. 2, pp. R1–R20, Apr. 2004.
[37] C. V. C. Bouten, K. T. M. Koekkoek, M. Verduin, R. Kodde, and J. D. Janssen, "A triaxial accelerometer and portable data processing unit for the assessment of daily physical activity," *IEEE Trans. Biomed. Eng.*, vol. 44, no. 3, pp. 136–147, Mar. 1997.
[38] J. Fahrenberg, F. Foerster, M. Smeja, and W. MüLler, "Assessment of posture and motion by multichannel piezoresistive accelerometer recordings," *Psychophysiology*, vol. 34, no. 5, pp. 607–612, Sep. 1997.
[39] A. M. Khan, Y.-K. Lee, S. Y. Lee, and T.-S. Kim, "A triaxial accelerometer-based physical-activity recognition via augmented-signal features and a hierarchical recognizer," *IEEE Trans. Inf. Technol. Biomed.*, vol. 14, no. 5, pp. 1166–1172, Sep. 2010.
[40] L. Sun, D. Zhang, B. Li, B. Guo, and S. Li, "Activity recognition on an accelerometer embedded mobile phone with varying positions and orientations," in *Proc. Int. Conf. Ubiquitous Intell. Comput.* Cham, Switzerland: Springer, 2010, pp. 548–562.
[41] O. Banos, J.-M. Galvez, M. Damas, H. Pomares, and I. Rojas, "Window size impact in human activity recognition," *Sensors*, vol. 14, no. 4, pp. 6474–6499, Apr. 2014.
[42] S. Lundberg and S. Lee, "A unified approach to interpreting model predictions," in *Proc. Adv. Neural Inf. Process. Syst.*, vol. 30, Long Beach, CA, USA, 2017, pp. 4765–4774.
[43] J. H. Friedman, "Greedy function approximation: A gradient boosting machine," *Ann. Statist.*, vol. 29, no. 5, pp. 1189–1232, Oct. 2001.
[44] D. J. Cook and N. C. Krishnan, *Activity Learning: Discovering, Recognizing, and Predicting Human Behavior From Sensor Data*. Hoboken, NJ, USA: Wiley, 2015.
[45] V. Dentamaro, V. Gattulli, D. Impedovo, and F. Manca, "Human activity recognition with smartphone-integrated sensors: A survey," *Expert Syst. Appl.*, vol. 246, Jul. 2024, Art. no. 123143.
[46] M. H. Arshad, M. Bilal, and A. Gani, "Human activity recognition: Review, taxonomy and open challenges," *Sensors*, vol. 22, no. 17, p. 6463, Aug. 2022.
[47] J. O'Halloran and E. Curry, "A comparison of deep learning models in human activity recognition and behavioural prediction on the MHEALTH Dataset," in *Proc. AICS*, 2019, pp. 212–223.
[48] M. Kaseris, I. Kostavelis, and S. Malassiotis, "A comprehensive survey on deep learning methods in human activity recognition," *Mach. Learn. Knowl. Extraction*, vol. 6, no. 2, pp. 842–876, Apr. 2024.
[49] G. Biau and E. Scornet, "A random forest guided tour," *TEST*, vol. 25, no. 2, pp. 197–227, Jun. 2016.
[50] Y. J. Luwe, C. P. Lee, and K. M. Lim, "Wearable sensor-based human activity recognition with ensemble learning: A comparison study," *Int. J. Electr. Comput. Eng. (IJECE)*, vol. 13, no. 4, p. 4029, Aug. 2023.
[51] T. Chen and C. Guestrin, "XGBoost: A scalable tree boosting system," in *Proc. 22nd ACM SIGKDD Int. Conf. Knowl. Discovery Data Mining*, Aug. 2016, pp. 785–794.
[52] GeeksforGeeks.(2024). *Difference Between Random Forest Vs Xgboost*. Accessed: Aug. 25, 2024. [Online]. Available: https://www.geeksforgeeks.org/difference-between-random-forest-vs-xgboost/
[53] D. A. Pisner and D. M. Schnyer, "Support vector machine," in *Machine Learning*. Amsterdam, The Netherlands: Elsevier, 2020, pp. 101–121.
[54] K. G. Manosha Chathuramali and R. Rodrigo, "Faster human activity recognition with SVM," in *Proc. Int. Conf. Adv. ICT Emerg. Regions (ICTer)*, Dec. 2012, pp. 197–203.
[55] Z. Chen, Q. Zhu, Y. C. Soh, and L. Zhang, "Robust human activity recognition using smartphone sensors via CT-PCA and online SVM," *IEEE Trans. Ind. Informat.*, vol. 13, no. 6, pp. 3070–3080, Dec. 2017.
[56] F. Hernández, L. F. Suárez, J. Villamizar, and M. Altuve, "Human activity recognition on smartphones using a bidirectional LSTM network," in *Proc. 22nd Symp. Image, Signal Process. Artif. Vis. (STSIVA)*, Bucaramanga, Colombia, Apr. 2019, pp. 1–5.
[57] W. E. Marcilio and D. M. Eler, "From explanations to feature selection: Assessing SHAP values as feature selection mechanism," in *Proc. 33rd SIBGRAPI Conf. Graph., Patterns Images (SIBGRAPI)*, 2020, pp. 340–347.
[58] J. Sundaram et al., "An exploration of Python libraries in machine learning models for data science," in *Proc. Adv. Interdiscipl. Appl. Mach. Learn. Python Libraries Data Sci.*, 2023, pp. 1–31.
[59] A. Name. (2023). *Scikit-learn Vs Tensorflow: Which One Should You Choose?*. Accessed: Oct. 6, 2023. [Online]. Available: https://www.example.com
[60] S. Ravindra. (2024). *Auc Roc Curve in Machine Learning*. [Online]. Available: https://www.geeksforgeeks.org/auc-roc-curve/
[61] S. Narkhede, "Understanding auc-roc curve," *Towards Data Sci.*, vol. 26, no. 1, pp. 220–227, 2018.
[62] S. Hochreiter, "Long short-term memory," in *Neural Computation*. Cambridge, MA, USA: MIT Press, 1997.
[63] T. Ajay. (2021). *Feature selection and dimensionality reduction*. [Online]. Available: https://www.linkedin.com/pulse/feature-selection-dimensionality-reduction-ajay-taneja/
[64] N. Ahmed, J. I. Rafiq, and M. R. Islam, "Enhanced human activity recognition based on smartphone sensor data using hybrid feature selection model," *Sensors*, vol. 20, no. 1, p. 317, Jan. 2020.
[65] F. Gu, M.-H. Chung, M. Chignell, S. Valaee, B. Zhou, and X. Liu, "A survey on deep learning for human activity recognition," *ACM Comput. Surveys (CSUR)*, vol. 54, no. 8, pp. 1–34, 2021.
[66] (2024). *Otii Arc Pro*. [Online]. Available: https://www.qoitech.com/products/otii/otii-arc-pro
[67] D. B. Ahmed, L. E. Díez Blanco, and E. M. Diaz, "Performance comparison of wearable-based pedestrian navigation systems in large areas," in *Proc. Int. Conf. Indoor Positioning Indoor Navigat. (IPIN)*, Sep. 2017, pp. 1–7.
[68] D. Anguita, A. Ghio, L. Oneto, X. Parra, and J. L. Reyes-Ortiz, "A public domain dataset for human activity recognition using smartphones," *Esann*, vol. 3, no. 1, pp. 437–442, 2013.
[69] M. Matey-Sanz, S. Casteleyn, and C. Granell, "Dataset of inertial measurements of smartphones and smartwatches for human activity recognition," *Data Brief*, vol. 51, Dec. 2023, Art. no. 109809.
[70] M. Matey-Sanz, S. Casteleyn, and C. Granell, "Smartphone and smartwatch inertial measurements from heterogeneous subjects for human activity recognition," *Data Brief*, vol. 48, 2023, Art. no. 109809.

Asiimwe Paddy Junior received the bachelor's degree in computer science, the master's degree in data communications and software engineering from Makerere University, Kampala, Uganda, in 2012, and 2016, respectively, and the Ph.D. degree in engineering for the information society and sustainable development (under the supervision of Luis Enrique Díez Blanco and Dr. Odongo Steven Eyobu) from the University of Deusto, Bilbao, Spain, in 2025.

He has been serving as an Assistant Lecturer and a Researcher with the Department of Information Systems, College of Computing and Information Science, Makerere University, since 2012. He joined the 6i Dirs COFUND Project in February 2021. He also works as a Research Assistant with DeustoTech—Instituto Tecnológico Deusto, University of Deusto, Bilbao. His research interests include wireless sensor networks, mobile application development, localization, ambient assisted living, and artificial intelligence.

Luis Enrique Díez received the bachelor's degree in telecommunications engineering from the University of Deusto, Bilbao, Spain, in 2005, the master's degree in communications technologies and systems from the Telecommunications Engineering School, Polytechnic University of Madrid, Madrid, Spain, in 2012, and the Ph.D. degree in engineering from the University of Deusto, in 2019.

From 2005 to 2011, he worked as a Senior IT Consultant at Everis, now NTT Data Spain, in their Madrid, Spain office. From 2013 to 2014, he joined the SOFTLAB Research Group, Carlos III University of Madrid (UC3M), Getafe, Spain, as a Research Support Technician. From 2014 to 2022, he worked as a Researcher at DeustoTech, the research institute of the engineering faculty of the University of Deusto. He currently works as an Assistant Professor with the Faculty of Engineering, University of Deusto, and is a member of the research group "Deusto Smart Mobility." He has worked (leading some of them) on more than ten regional, national, and international research projects and contracts. He has co-authored 15 research manuscripts published in international journals and more than ten communications in international congresses. His interests include signal processing and data fusion for the development of location-based services, ambient assisted living, and intelligent environments.

Alfonso Bahillo received the bachelor's degree in telecommunications engineering and the Ph.D. degree from the University of Valladolid, Valladolid, Spain, in 2006 and 2010, respectively.

He has the PMP Certification with PMI, in 2014. From 2006 to 2010, he joined CEDETEL as a Research Engineer. From 2006 to 2011, he was an Assistant Professor at the University of Valladolid. From 2013 to 2017, he held a post-doctoral position, and from 2017 to 2020, the Director of DeustoTech-Fundacion Deusto, University of Deusto, Bilbao, Spain. Currently, he is an Associate Professor at the University of Valladolid. He has worked (leading some of them) in more than 25 regional, national, and international research projects and contracts. He has co-authored more than 35 research papers, published in international journals, more than 40 communications in international conferences, and four national patents. His interests include local and global positioning techniques, ambient assisted living, biomedical and health informatics, and wireless networking.

Odongo Steven Eyobu received the B.Sc. degree in computer science from Islamic University, Mbale, Uganda, in 2004, the M.Sc. degree in data communication and software engineering from Makerere University, Kampala, Uganda, in 2007, and the Ph.D. degree in electronics engineering from Kyungpook National University, Daegu, South Korea, in 2018.

He is currently a Senior Lecturer with the School of Computing and Informatics Technology, Makerere University. His research interests include deep learning systems, indoor localization, vehicular communications, intelligent transportation systems, and wireless sensors.